FDL-TDR-64-125

STRESS ANALYSIS OF A PARACHUTE DURING INFLATION AND AT STEADY STATE

HELMUT G. HEINRICH
LELAN R. JAMISON, JR.

FOREWORD

This report was prepared by the staff and students of the Department of Aeronautics and Engineering Mechanics of the University of Minnesota in compliance with USAF Contract No. AF33(657)-11184, Project No. 6065, Task No. 606503, "Theoretical Parachute Investigation." Work under this investigation was accomplished during this period April 1963 to August 1964. Work being accomplished under this contract is sponsored jointly by U. S. Army Natick Laboratories, Department of the Army; Bureau of Naval Weapons, Department of the Navy; and Air Force Systems Command, United States Air Force, and is directed by a Tri-Service Steering Committee concerned with Aerodynamic Retardation. Contract administration has been conducted by Research and Technology Division (RTD); and Messrs. Rudi J. Berndt and James H. DeWeese of the Air Force Flight Dynamics Laboratory have been project engineers.

The publication of this report does not constitute approval by the Air Force of the findings or conclusions contained herein. It is published only for the exchange and stimulation of ideas.

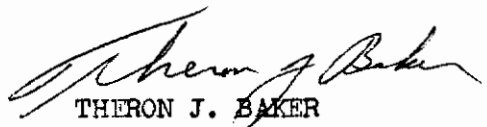

THERON J. BAKER
Vehicle Equipment Division
AF Flight Dynamics Laboratory

ABSTRACT

The stresses occurring in the cloth of an opening parachute and at steady state are calculated. The method is based on assumed instantaneous and steady state shapes and related pressure distributions. It is general and may be applied to any type and size of canopy built out of solid cloth. The presented analysis is limited to canopies constructed of triangular gores, but can be extended to other gore patterns. A numerical calculation is made for the Solid Flat, Circular Parachute during the opening and at steady state.

TABLE OF CONTENTS

ILLUSTRATIONS

ILLUSTRATIONS (Cont.)

SYMBOLS

b_o	a length (see Figs 2 and 5)
C_D	drag coefficient
C_{D_o}	drag coefficient based on canopy nominal area
$(C_DS)_s$	drag area of store
C_p	pressure coefficient
D	diameter
D_c	cord-line profile projected diameter
D_o	canopy nominal diameter
D_v	vent diameter
d_o	a length (see Fig 5)
E	cloth modulus of elasticity (lb/ft)
f_1	circumferential stress (lbs/ft; see Fig 3)
f_2	meridional stress (lbs/ft; see Fig 3)
g	acceleration of gravity (ft/sec^2)
F	force between canopy and store (see Fig 2)
F_{max}	opening force or opening shock
N	number of gores
plane Q	(illustrated in Fig 3)
Δ p	pressure differential across cloth (see Fig 5)
q	dynamic pressure = $\frac{1}{2}\rho V^2$
r_b	bulge radius (see Figs 3 and 5)
S	area

SYMBOLS (cont.)

S_o	canopy nominal area
s	a length (see Figs 2, 3 and 6)
t	time
t_f	filling time
V	velocity
V_o	launch velocity
W_s	store weight
x	a length (see Figs 2 and 3)
y	a length (see Fig 5)
z	a length (see Fig 2)
α	gore half-angle (see Fig 5)
δ	an angle (see Fig 4)
ε	strain
θ	angle of suspension lines from canopy centerline (see Fig 2)
λ^*	a dimensionless parameter (see Eqn 23)
ρ	radius of curvature (see Figs 3 and 4)
ϕ	an angle (see Fig 2)

SUPERSCRIPTS

*	a dimensionless quantity

SYMBOLS (cont.)

SUBSCRIPTS

o	initial or unstretched condition
c	referred to cord line
g	referred to gore centerline
∞	free stream conditions

1. INTRODUCTION

A review of the available literature on the parachute canopy stresses reveals that all previous attempts have been limited to treating the steady descent case.

The earliest analytical studies of the parachute stress problem, which were summarized by Jones in 1923 (Ref 1), seem to have been made by the British investigators Taylor, Southwell, Griffiths, Jones and Williams. This early work was limited to a study of canopy shapes assuming an infinite number of gores in which the stresses thus approach a limit of zero.

In 1942 Stevens and Jones re-examined the basic analysis and studied the case where the number of lines is finite (Ref 2). This study is primarily concerned with canopy shapes, but also concludes that cloth stresses should be only circumferential. They also predicted, unlike the original work, that the stresses at the canopy apex should not be infinite. This agreed with another analysis made by Duncan, Stevens and Richards (Ref 3) which showed that the stresses at the apex of the parachute are not infinite if the elasticity of the fabric is taken into account.

German work on parachute stresses has dealt with surfaces of revolution. Beck (Ref 4) derived expressions for the membrane stresses in a variety of shells of revolution for pressures both constant and linearly varying. Reagen (Ref 5) in the United States also considered parachutes as surfaces of revolution.

Finally, Topping, Marketos and Costakos at Goodyear Aircraft Corporation (Ref 6) studied parachute stresses as part of a larger investigation of canopy shapes. Their method of approach was to apply a modified form of membrane theory to canopy shapes obtained from photographs. This method requires an exact knowledge of the distance between the cord lines over the canopy and the centerline of the inflated gores. Unfortunately, a photograph gives a profile view of the inflated gore centerlines, but reveals little about the position of the cord lines. The required distance may be measured from the photograph only at the skirt where the suspension lines join the canopy. Thus, in Ref 6 only the stresses in the skirt region were calculated. The authors

Manuscript released by authors August 1964 for publication as an ASD Technical Documentary Report.

then made the assumption that the stresses over most of the remaining portion of the canopy are constant and equal to the one at the skirt. This, by the admission of the authors, left much to be desired but was the best approximation they felt could be made at that time. The method presented in Ref 6 is also limited to the steady state or fully inflated parachute condition.

The approach chosen in the following study is based on the profile picture of a fully inflated parachute for the steady state case and on intermediate forms during the period of inflation. From the profile picture which represents the curvature of the gore centerline, the cord profile can be calculated if the flat gore pattern is known. From the gore centerline and cord profile, in combination with the flat gore pattern, the free span between the suspension lines and the bulge radius of the gore can be calculated. With span and radius known, the stress in the cloth depends merely on the pressure differential and the material's elasticity. Since the profile under steady state condition is well known for conventional parachutes, or can easily be obtained for any type, this method should provide very realistic values of the stress distribution over the entire canopy.

The same concept is also utilized to calculate the stress during the opening. However, for this period intermediate canopy shapes are assumed identical to those which are used in the parachute opening theory based on the mass balance first proposed by O'Hara (Ref 7). This has the advantage that these intermediate forms are relatively simple, can be described mathematically, and also that the stress analysis can be coupled with an opening shock calculation which provides the required instantaneous pressure differential. In this manner a realistic stress calculation can be performed on an analytical basis. The process can also be reversed by assuming a cord line profile and calculating the profile of the gore centerline. The details of this general method will be shown in the following chapters.

Finally, the authors wish to express their appreciation to the students of Aero-Space Engineering at the University of Minnesota who participated in this research project, and in particular to Mr. Daryl J. Monson (Ref 8).

2. THE CANOPY PROFILE

The gores of a parachute during inflation and at steady descent bulge out between adjacent cord lines as shown in Fig 1. The profile view of a typical canopy shape at some instant is shown in Fig 2. Related to these profiles, one can define an incremental element of an inflated gore as shown in Figs 2 and 3. The element lies in a plane Q which is normal to the gore centerline.

The following simplifying assumptions shall now be made:

1. At any instant of opening and at steady state, the pressure difference may vary over the canopy in the meridional direction, but is constant circumferentially, i.e., axisymmetric. This assumption was also made in Ref 6.

2. The stresses in the cloth occur in the circumferential direction only. These are shown as f_1 in Fig 3. The meridional stresses, f_2, are negligibly small. Reference 1 and other sources also made this assumption for the steady-state case. This assumption also appears reasonable for the period of inflation and the functioning of Ribbon and Ringslot parachutes may be considered as experimental proof.

3. The cross-sectional shape in a plane Q of any gore element is a circular arc because of uniform pressure distribution over the element (Ref 9). The arc cannot exceed a semicircle, since adjacent gores would then interfere with each other as is observed from Fig 1. When the calculations indicate excess cloth, the cross section is treated as a semicircle with parallel extension to the cords. This concept is particularly important for the parachute during the early stages of inflation.

4. Inertial forces and related stresses of the gore element which may occur during the inflation are neglected because it would be very difficult to represent these realistically and there is no experimental evidence of their significance.

In view of these basic assumptions, Figs 4 and 5 show an enlarged gore and cord-line element with and without the cord lines, respectively.

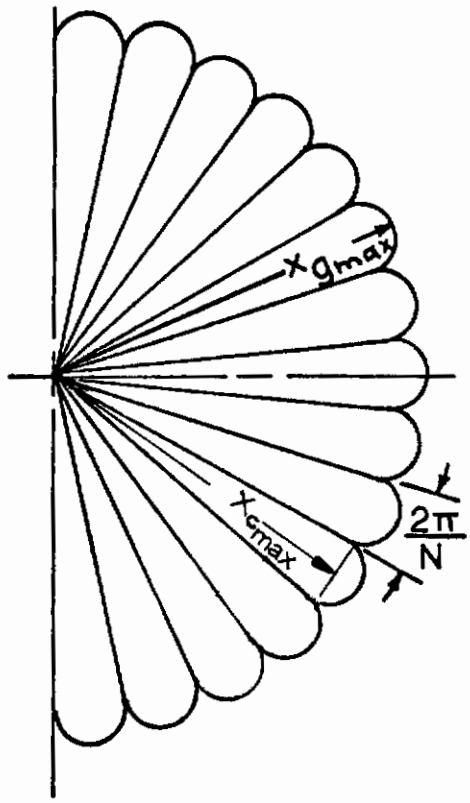

FIG 1 - TOP VIEW OF AN INFLATING CANOPY AT SOME INSTANT

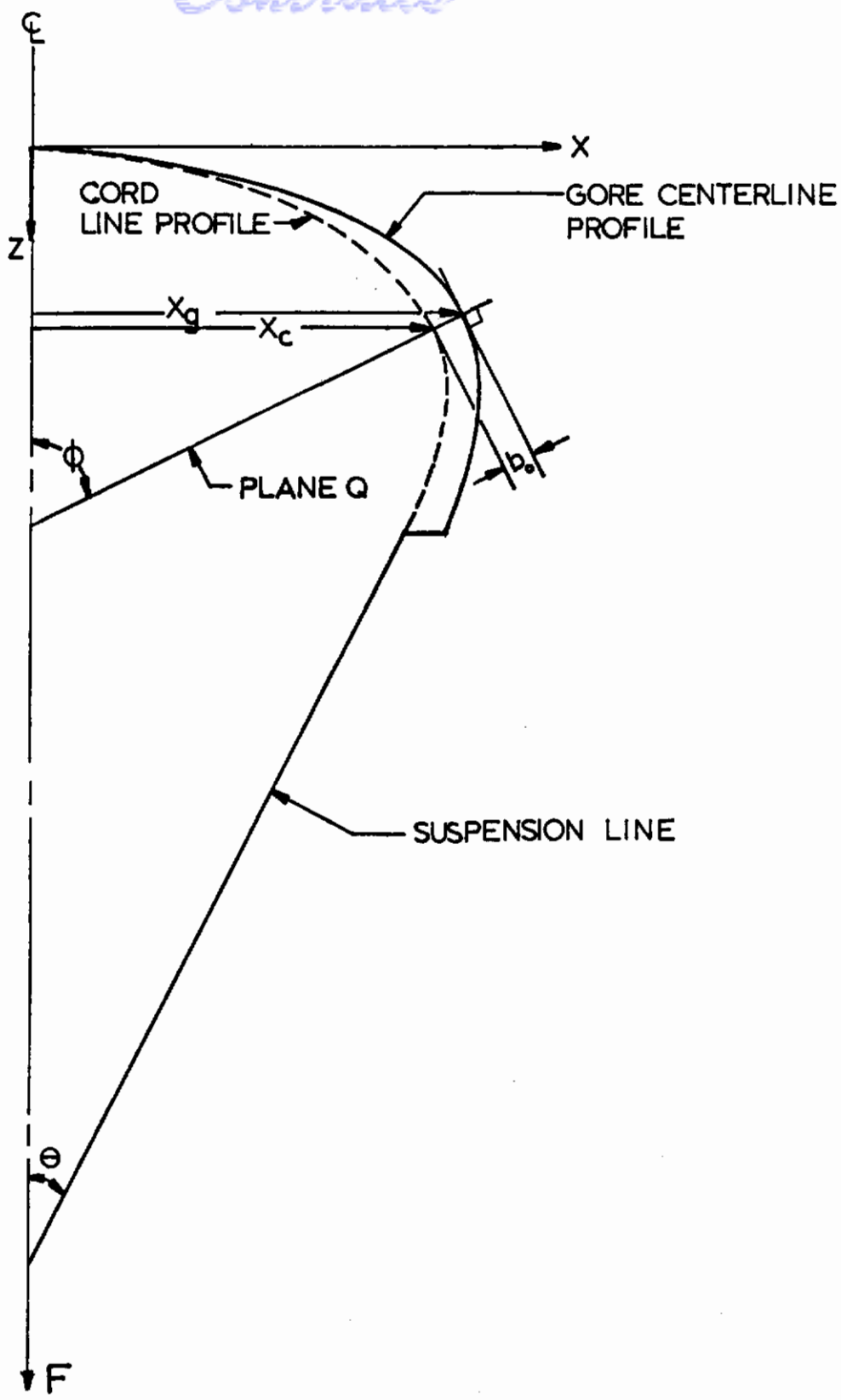

FIG 2 PROFILE VIEW OF A CANOPY AT SOME INSTANT OF OPENING

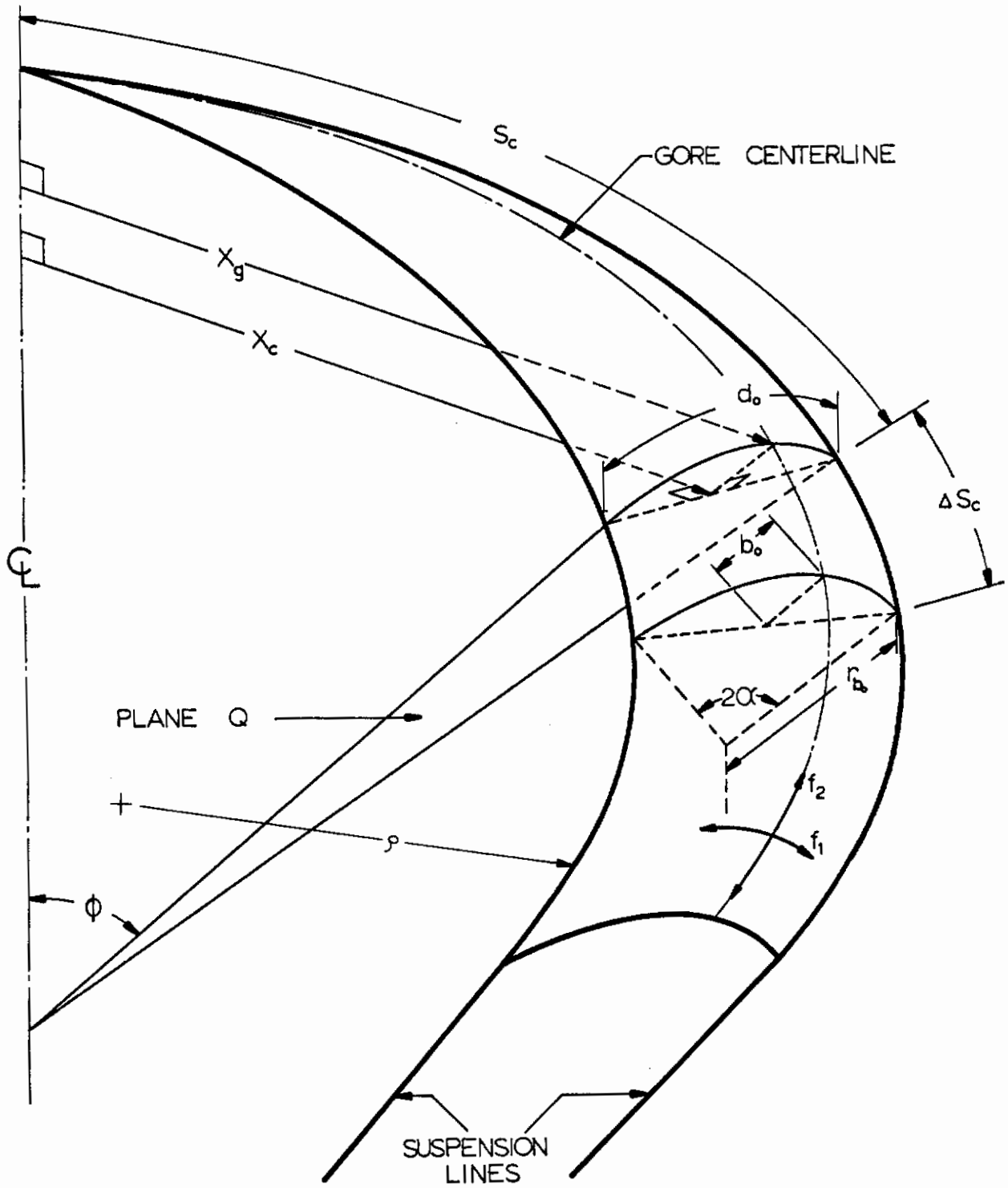

FIG 3. DETAIL VIEW OF A TYPICAL GORE DURING INFLATION

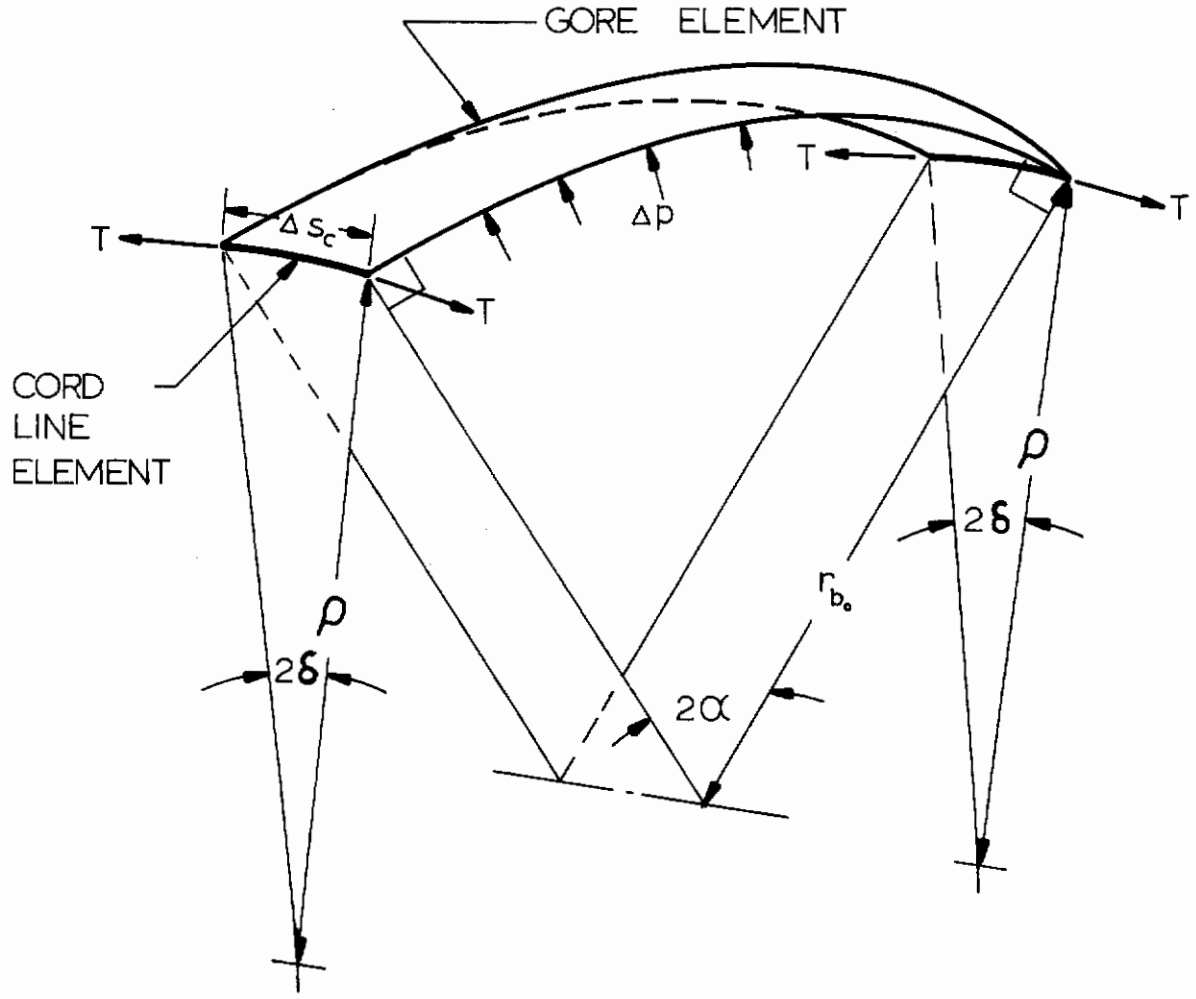

FIG 4. DETAIL VIEW OF A TYPICAL GORE AND CORD-LINE ELEMENT SHOWING THE APPLIED FORCES

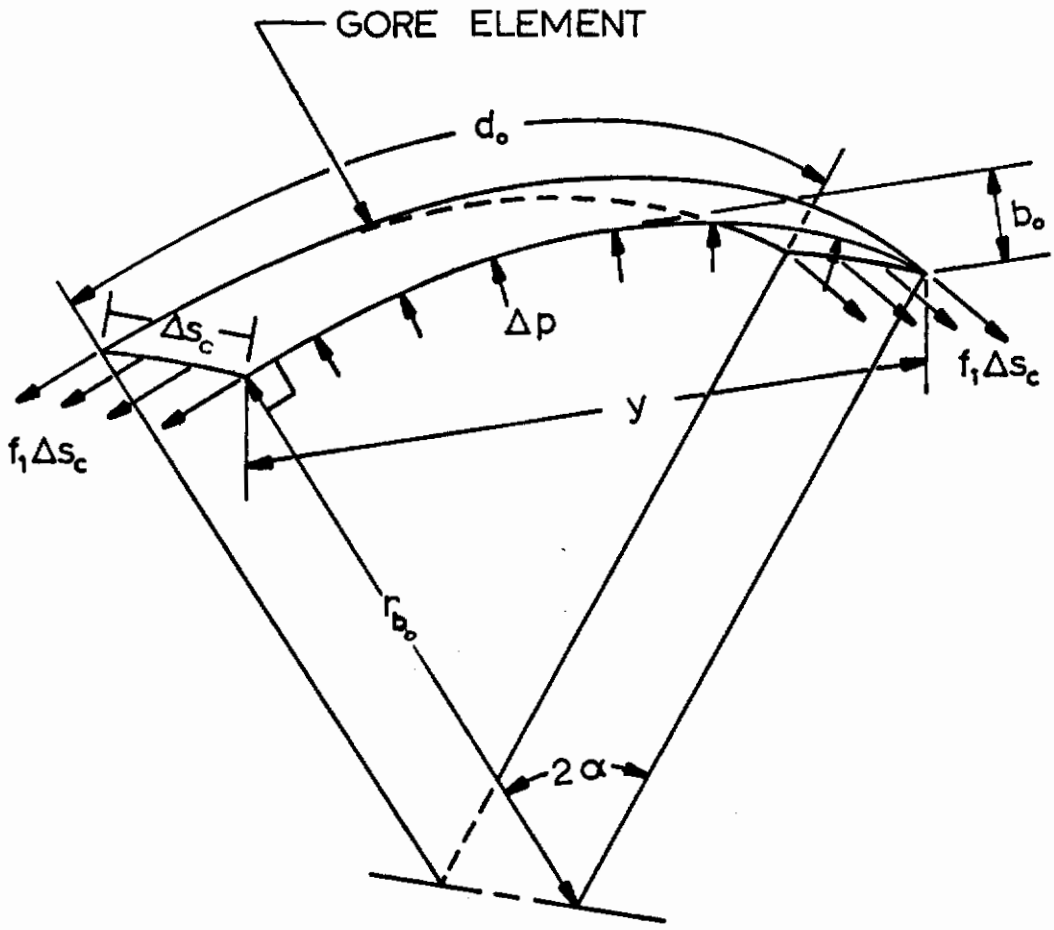

FIG 5 DETAIL VIEW OF A TYPICAL GORE ELEMENT SHOWING THE APPLIED FORCES

3. DETERMINATION OF THE CORD-LINE PROFILE

The bulge radius, r_{b_o}, and the pressure differential, Δp, determine in principle the local stress. Unfortunately, the opacity of the parachute canopy hides the cord lines in a photograph, revealing only the gore centerline profile. Therefore, an attempt shall be made to obtain the cord-line profile for a parachute with triangular gore pattern from a known or reasonably assumed gore centerline profile. In the first approximation, the cloth and cord lines are considered to be inextensible for the purpose of obtaining the cord-line profile. (This is indicated by the subscript "o".) Later, in the stress equation, the elasticity of the cloth will be considered, but for this case it may be neglected since it is usually small and affects the cord-line position only to a minor degree. This method is general and the fully inflated canopy is merely a special case.

In Figs 2 and 5, the length b_o, lying in plane Q, is the distance between the gore centerline and the midpoint of the line connecting the adjacent cord lines. As a first step, the length b_o shall be expressed in terms of known quantities, which allows the determination of the cord-line profile by simply measuring off b_o inward from the gore centerline.

From Fig 5 follows:

$$y = 2r_{b_o} \sin \alpha_o = 2r_{b_o} \left(\alpha_o - \frac{\alpha_o^3}{3!} + \ldots \right) \qquad (1)$$

and

$$d_o = 2r_{b_o} \alpha_o \, . \qquad (2)$$

In addition, it may be written that

$$b_o = r_{b_o} (1-\cos \alpha_o) = r_{b_o} \left(1-1+ \frac{\alpha_o^2}{2!} - \frac{\alpha_o^4}{4!} + \ldots \right). \qquad (3)$$

In Eqns 1 and 3, $\sin \alpha_o$ and $\cos \alpha_o$ have been expanded in series form. It will later be seen that this form is a very convenient one and sufficient accuracy is maintained with the indicated terms.

A typical flat gore is shown in Fig 6, for which one sets:

$$d_o = 2 S_g \tan \frac{\pi}{N} , \qquad (4)$$

where N is the number of gores.

Also, from Figs 2, 3 and 5 it can be seen that

$$y = 2x_c \tan \frac{\pi}{N} . \qquad (5)$$

In view of the basic concept, namely that merely the profile of the gore centerline is known, the term x_c in Eqn 5 is unknown and a further relation is necessary.

From Figs 2 and 3 follows:

$$x_c = x_g - b_o \sin \phi . \qquad (6)$$

These six equations contain six unknowns--y, r_{b_o}, α_o, b_o, d_o and x_c. Since the remaining quantities, N, x_g, s_g, and ϕ are known, it is possible to solve the system of equations for b_o, which is sufficient to determine the cord-line profile.

It has been found, however, that the equation for b_o becomes very cumbersome when expressed in the known terms of x_g and s_g. The solution in terms of x_c and s_g is much simpler, and after considerable algebraic manipulations one obtains:

$$b_o = \frac{\sqrt{6} \tan \frac{\pi}{N}}{4 \sqrt{s_g}} (s_g - x_c)^{\frac{1}{2}} (s_g + x_c). \qquad (7)$$

The detailed steps of this derivation are shown in Appendix I.

This equation includes the so-far unknown term x_c. However, it will be seen that for most practical cases $x_c \approx x_g$, and if this is unsatisfactory a certain iteration process can be performed which quickly converges. Details of this matter will be discussed at the end of this chapter.

In accordance with Assumption 3, p. 9, Eqn 7 will be valid as long as the gore element forms an arc equal to or less than a semicircle. When the gore is bulged out in

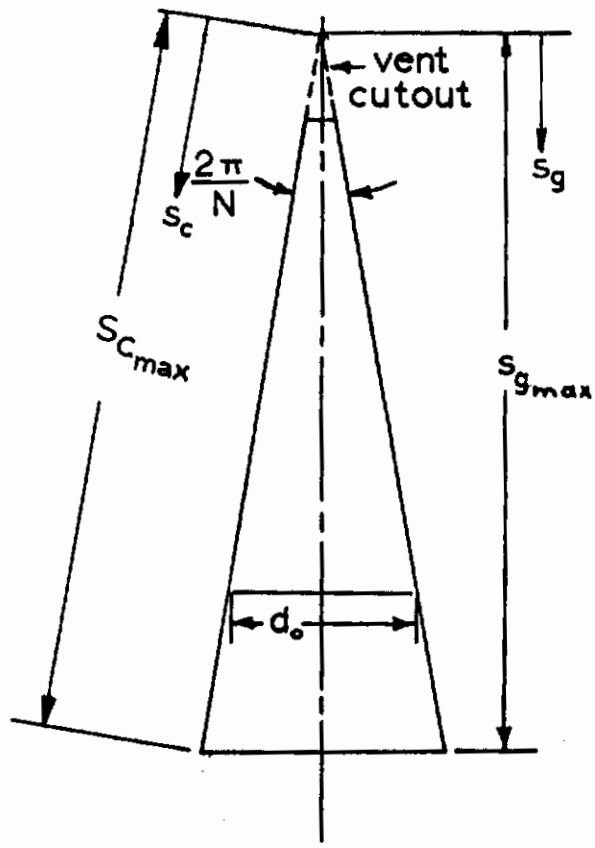

FIG 6 TRIANGULAR GORE PATTERN FOR A SOLID FLAT CANOPY

the shape of a semicircle with parallel extension, the geometry of Fig 5 indicates that in such a case

$$b_o = \frac{y}{2} + \frac{1}{2}\left(d_o - \frac{\pi}{2} y\right) = \frac{1}{2}\left[d_o + \left(1 - \frac{\pi}{2}\right) y\right] = \tan\frac{\pi}{N}\left[s_g + \left(1 - \frac{\pi}{2}\right) x_c\right] , \quad (8)$$

where the last step results from substitution of Eqns 4 and 5. Finally, expressing b_o in terms of x_g and s_g by means of Eqn 6, gives:

$$b_o = \frac{\tan\frac{\pi}{N}\left[s_g + \left(1 - \frac{\pi}{2}\right) x_g\right]}{1 + \tan\frac{\pi}{N}\left(1 - \frac{\pi}{2}\right)\sin\phi} \quad (9)$$

For the practical solution of the problem it is necessary to determine which equation has to be used for the calculation of b_o. For this purpose, the following criterion shall be established. Figure 5 shows that an arc less than a semicircle occurs if

$$d_o < \frac{\pi}{2} y . \quad (10)$$

Substitution of Eqns 4 and 5 for d_o and y gives the above inequality as

$$\frac{2 s_g}{\pi x_c} < 1 . \quad (11)$$

The term x_c may be replaced by Eqn 6 to give

$$\frac{2 s_g}{\pi (x_g - b_o \sin\phi)} < 1 , \quad (11a)$$

and under this condition b_o must be calculated from Eqn 7.

From Eqn 11a it can be seen that if the inequality is reversed to

$$\frac{2 s_g}{\pi (x_g - b_o \sin\phi)} \geq 1, \quad (12)$$

then, for this case, Eqn 9 should be used to calculate b_o. Substituting b_o by means of Eqn 9 into Eqn 12 gives, after some manipulation,

$$\frac{\frac{2 s_g}{\pi}\left[1 + \tan\frac{\pi}{N}\sin\phi\left(1 - \frac{\pi}{2}\right)\right]}{x_g - \sin\phi\, s_g \tan\frac{\pi}{N}} \geq 1. \quad (13)$$

Now Eqn 13 is expressed in terms of known quantities and, in summary, it may be stated that b_o should be calculated in accordance with the following criterion:

$$\text{if} \quad \frac{\frac{2s_g}{\pi}\left[1 + \tan\frac{\pi}{N}\sin\phi\,(1 - \frac{\pi}{2})\right]}{x_g - \sin\phi\tan\frac{\pi}{N}s_g} \;\Bigg|\; \begin{array}{l} < 1, \text{ apply Eqn 7} \\ \geqslant 1, \text{ apply Eqn 9.} \end{array} \tag{14}$$

In order to make the preceding equations more universal, they can be made dimensionless by means of the nominal parachute diameter, D_o, and one obtains:

$$b_o^* = \frac{b_o}{D_o/2}\,, \quad x_c^* = \frac{x_c}{D_o/2}\,, \quad s_c^* = \frac{s_c}{D_o/2}\,,$$

$$x_g^* = \frac{x_g}{D_o/2}\,, \quad \text{and} \quad s_g^* = \frac{s_g}{D_o/2}\,. \tag{15}$$

In dimensionless form, Eqn 7, 6, 9 and 14 become, respectively:

$$b_o^* = \frac{\sqrt{6}\tan\frac{\pi}{N}}{4\sqrt{s_g^*}}\,(s_g^* - x_c^*)^{\frac{1}{2}}\,(s_g^* + x_c^*) \tag{7a}$$

$$x_c^* = x_g^* - b_o^*\sin\phi \tag{6a}$$

$$b_o^* = \frac{\tan\frac{\pi}{N}\left[s_g^* + (1 - \frac{\pi}{2})\,x_g^*\right]}{1 + \tan\frac{\pi}{N}(1 - \frac{\pi}{2})\sin\phi} \tag{9a}$$

and if

$$\frac{2\,s_g^*\left[1 + \tan\frac{\pi}{N}\sin\phi\,(1 - \frac{\pi}{2})\right]}{x_g^* - s_g^*\sin\phi\tan\frac{\pi}{N}} \;\Bigg|\; \begin{array}{l} < 1, \text{ apply Eqn 7a} \\ \geqslant 1, \text{ apply Eqn 9a.} \end{array} \tag{14a}$$

The actual procedure to find the significant canopy parameters which ultimately will lead to the determination of the stress distribution may now be described as follows.

1. Establish from available photographs or by other means the profile of the gore centerline.

2. Erect at several values of s_g the normal to the gore centerline profile and extend these lines to the canopy centerline. These lines are the traces of the planes Q, as shown in Figs 2 and 3.

3. Determine the distances x_g^* and s_g^* and the angle ϕ related to each value of s_g on the gore centerline.

4. Determine which equation for b_o applies from inequality 14a.

5. Calculate b_o^* from either Eqn 7a or Eqn 9a. If Eqn 7a is used, calculate a first approximation for b_o^* by using x_g^* in place of x_c^*. In many cases where $\frac{N}{D_o}$ is large, for example $N/D_o \geq 1.0$, this gives sufficient accuracy. If $\frac{N}{D_o}$ is small or if better accuracy is needed, the first approximation for b_o^* can be used in Eqn 6a to find x_c^*. By using Eqns 6a and 7a in this manner, an iteration process can be applied until a value for b_o^* is obtained that satisfies both equations.

6. Lay off the final values for b_o^* in the planes Q and construct the cord-line profiles.

These steps complete the canopy geometry.

4. THE EQUATION FOR CLOTH STRESSES

The basic equation relating cloth stress to the pressure differential and the gore bulge is (Ref 10):

$$f_1 = \Delta p r_b \tag{16}$$

In order to obtain the cord-line profile, the cloth was assumed inextensible. This requirement is now dropped and it shall be assumed instead that the cloth is perfectly elastic, obeying Hook's Law. It follows that

$$f_1 = E \varepsilon \quad . \tag{17}$$

It is known, however, that parachute cloth, particularly nylon material, deviates from this ideal behavior. But to keep the analysis simple, E may be taken in the first approximation as a constant, equal to the ratio of the failure stress to the failure strain. This approximation appears to be acceptable, particularly if the cloth is not stressed up to its ultimate strength.

Mention should be made of the effect of using cloth cut as bias weave as compared to straight weave. Bias weave has approximately the same failure stress as straight weave but approximately twice the failure strain. Thus, E for bias weave can be seen to be about one-half of the E for straight weave. Use of bias weave leads to better energy absorption, to a reduction of stress due to larger cloth extension which may result in a reduction of the bulge radius, r_b, and to a certain equalization of the stresses in case of seams and other discontinuities.

If it can be assumed that the strain is constant over any gore element, one may write from the conventional definition of strain and from observation of Figs 5 and 6 that

$$\varepsilon = \frac{\Delta d}{d_o} = \frac{d - d_o}{d_o} \quad ,$$

or

$$d = (1 + \varepsilon)\, d_o \quad . \tag{18}$$

Equations 16, 17 and 18, in addition to the previously derived Eqns 1 and 2, constitute a system of five

equations involving the five unknowns f_1, r_b, α, d, and ε. In Eqns 1 and 2, the subscript "o" is now removed since the cloth is assumed to be extensible.

Notice that once again sin α is expanded in series form in Eqn 1. The series is terminated after two terms, since this has been found to give sufficient accuracy in all cases. A maximum error of 7.5% is introduced if α achieves 90°. Since α is considerably less than 90° over most of the canopy, the actual error is also much less than 7.5%. Furthermore, any error overestimates the stress which is desirable from a design and safety standpoint.

A solution of the given system of equations for the stress provides

$$f_1^3 + \left[\frac{6E^2\left(1-\frac{x_c}{s_g}\right) - 3E\left(\Delta p\, s_g \tan\frac{\pi}{N}\right)^2}{6E^2 - \left(\Delta p\, s_g \tan\frac{\pi}{N}\right)^2}\right] f_1^2 -$$

$$\left[\frac{3E^2\left(\Delta p\, s_g \tan\frac{\pi}{N}\right)^2}{6E^2 - \left(\Delta p\, s_g \tan\frac{\pi}{N}\right)^2}\right] f_1 - \left[\frac{E^3\left(\Delta p\, s_g \tan\frac{\pi}{N}\right)^2}{6E^2 - \left(\Delta p\, s_g \tan\frac{\pi}{N}\right)^2}\right] = 0. \qquad (19)$$

Details of this derivation are presented in the appendix.

Equation 19 is valid only as long as $\alpha < 90°$. If $\alpha = 90°$, b_o must be calculated from Eqn 9a and the resulting stress and strain can be calculated as hoop stress of a semicircle:

$$f_1 = \Delta p\, x_c \tan\frac{\pi}{N} \quad . \qquad (20)$$

More useful and workable equations for calculating the stress will result if they are made dimensionless.

Reviewing Eqn 19, one observes a common group of terms in the coefficients of ε. Therefore, it is useful at this time to introduce a dimensionless term, λ^*, defined as

$$\lambda^* = \Delta p \frac{D_o/2}{E} \tan\frac{\pi}{N} \quad , \qquad (21)$$

which abbreviates the equation. Finally, all lengths are made dimensionless, as shown previously by Eqn 15.

Substitution of Eqns 15, 17 and 21 into Eqns 19 and 20 gives, respectively

$$\varepsilon^3 + \left[\frac{6\left(1 - \frac{x_c^*}{s_g^*}\right) - 3(\lambda^* s_g^*)^2}{6 - (\lambda^* s_g^*)^2}\right] \varepsilon^2 - \left[\frac{3(\lambda^* s_g^*)^2}{6-(\lambda^* s_g^*)^2}\right] \varepsilon - \left[\frac{(\lambda^* s_g^*)^2}{6 - (\lambda^* s_g^*)^2}\right] = 0. \qquad (19a)$$

$$\varepsilon = \lambda^* x_c^* \quad . \qquad (20a)$$

Notice that the only way in which the design parameters of the parachute appear in Eqns 19a and 20a is through the dimensionless parameter, λ^*. This makes it possible to obtain for any given canopy shape a family of ε versus s_g^* curves with λ^* as a parameter. In other words, for the Solid Flat Parachute type, any combination of parachute characteristics resulting in the same value of λ^* will give the same strain, ε. This statement, however, includes also the requirement for identical gore centerline profiles which, for example, could be altered in spite of identical gore patterns through a variation of the relative length of the suspension lines.

The parameter λ^* includes the pressure differential Δp and for the further treatment this term must be determined.

Because of its complexity, the possibility of an analytical determination of the flow pattern, particularly during inflation, must be disregarded at this time. Experimentally, the pressure distribution could be measured by means of transducers which could be attached at various locations to the canopy. However, to date no pertinent information is available.

Another possibility is the experimental pressure determination by means of fixed shapes which are characteristic for the opening process. These shapes can be repre-

sented through rigid models suitable for conventional wind tunnel tests. These tests will yield a pressure coefficient, C_p, over the surfaces, which is defined as:

$$C_p = \frac{\Delta p}{q_\infty} \quad , \tag{22}$$

where q_∞ is the dynamic pressure. Details of these forms and pressure distribution are given in Ref 10.

In order to find the magnitude of the pressure differential of the inflating canopy, it is now merely necessary to know the free stream velocity and the related projected diameter. This information can be obtained from a simultaneously performed opening shock calculation or from an experimentally established velocity-shape-time relationship.

In this study experimental data as illustrated in Figs 16 and 17 will be used, for reasons of simplicity.

It must be realized that this method neglects a number of conditions which are connected with the dynamics of the opening process. However, it is safe to assume that at least in subsonic flow and excluding conditions of extremely fast inflation, this method should provide a good first order approximation.

After this preparation, λ^* can be determined. With this completed, the following outlined steps should be followed to obtain a complete numerical solution, first of the strain and then of the stress.

1. It is assumed that the cord-line and the gore centerline profiles are known for different stages of opening. The first step, then, is to determine λ^* for selected values of x_c^* and s_g^*.

2. From Eqn 14a determine whether α is less than or equal to 90°, which determines whether or not the strain, ε, shall be calculated from Eqn 19a or Eqn 20a, respectively.

3. Equation 19a could be solved by means of methods for the solution of cubic equations. However, this is cumbersome and an iteration process leads more quickly to satisfactory results. Equation 20a indicates the order of

magnitude of the strain involved in Eqn 19a and an iteration process can be performed until Eqn 19a is satisfied. A form sheet is shown in Fig 7, which may be used in the suggested iteration process.

4. After ϵ is known, the stress can be calculated from Eqn 17.

EQN. 19a: $\varepsilon^3 + \left\{ \frac{6\,(1 - x_c^*/s_g^*) - 3(\lambda^* s_g^*)^2}{6 - (\lambda^* s_g^*)^2} \right\} \varepsilon^2 - \left\{ \frac{3(\lambda^* s_g^*)^2}{6 - (\lambda^* s_g^*)^2} \right\} \varepsilon - \frac{(\lambda^* s_g^*)^2}{6 - (\lambda^* s_g^*)^2} = 0$

EQN. 21: $\lambda^* = \Delta p \frac{D_o/2}{E} \tan \frac{\pi}{N}$

EQN. 20a: $\varepsilon = \lambda^* x_c^*$

MODEL _____, $t^* =$ _____.

	EQN. 21															
①	ΔP															
②	$\frac{D_o/2}{E}$															
③	①·②															
④	③·tan $\frac{\pi}{N}$															
	EQN. 19a															
⑤	$\lambda^* \equiv$ ④															
⑥	$1 - x_c^*/s_g^* = 1 -$ ③															
⑦	6·⑥															
⑧	$\lambda^* s_g^* =$ ⑤·①															
⑨	$⑧^2$															
⑩	6 - ⑨															
⑪	3 · ⑨															
⑫	⑦-⑪															
⑬	⑫/⑩ (coeff. of ε^2)															
⑭	-⑪/⑩ (coeff. of ε)															
⑮	-⑨/⑩ (coeff. of 1)															
	EQN. 20a															
⑯	$\lambda^* x_c^* =$ ⑤·②															
⑰	$\varepsilon = f_1/E$															

FIG 7 OUTLINE OF STEPS TO OBTAIN STRAIN USING EQNS. 19a OR 20a

5. ILLUSTRATIVE EXAMPLE

The theory of the preceding sections will now be illustrated through the stress calculation for the case of the opening process and the steady state of a solid flat circular parachute canopy. For this purpose a parachute model was chosen which was also used in opening studies in the subsonic wind tunnel of the University of Minnesota. The characteristics of this model are as follows:

Number of gores, N = 28

Nominal diameter, D_o = 3 ft

Canopy area, S_o = 7.06 sq ft

Canopy material = 1.1 oz nylon, MIL-C-7020B

Modulus of elasticity, E = 2,180 lb/ft

Vent diameter D_v/D_o = 0.10.

It may now be assumed that this parachute goes, during the period of inflation, through the intermediate stages as shown in Figs 8 through 14. These shapes are chosen because their respective pressure distribution is known (Ref 10). The Figs 8 through 14 indicate the cord-line profile as well as the gore centerline profile. The cord lines were given by the existing wind tunnel models, whereas the gore centerlines were calculated in accordance with the preceding Section 3, under the assumption that the illustrated cord lines are representative for a solid flat circular parachute with 28 gores.

It should be noticed that this procedure differs from the previously described method, since here the profiles of the cord lines are assumed to be known and the gore centerlines are calculated. For this case, x_c is known. However, to solve either Eqn 7a or Eqn 9a, whichever is applicable, the gore centerline length, s_g^*, must be known. For the case of triangular gores, and referring again to Fig 6, s_g^* can be determined easily from

$$s_g^* = s_c^* \cos\left(\frac{\pi}{N}\right). \tag{23}$$

In Section 3 the process was reversed. Reviewing the theory and this illustrative example, however, it is

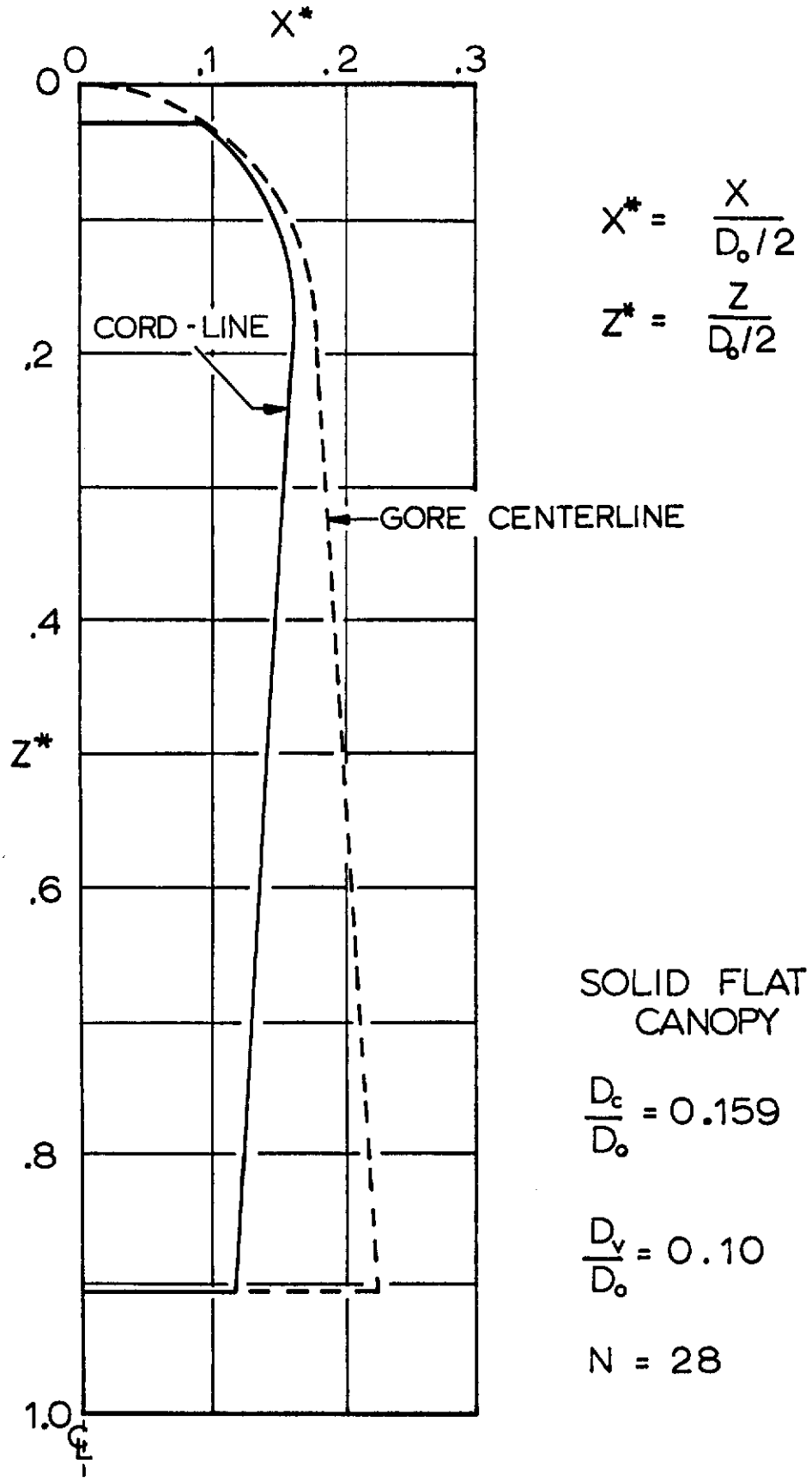

FIG 8 PROFILE SHAPE OF RIGID MODEL 1

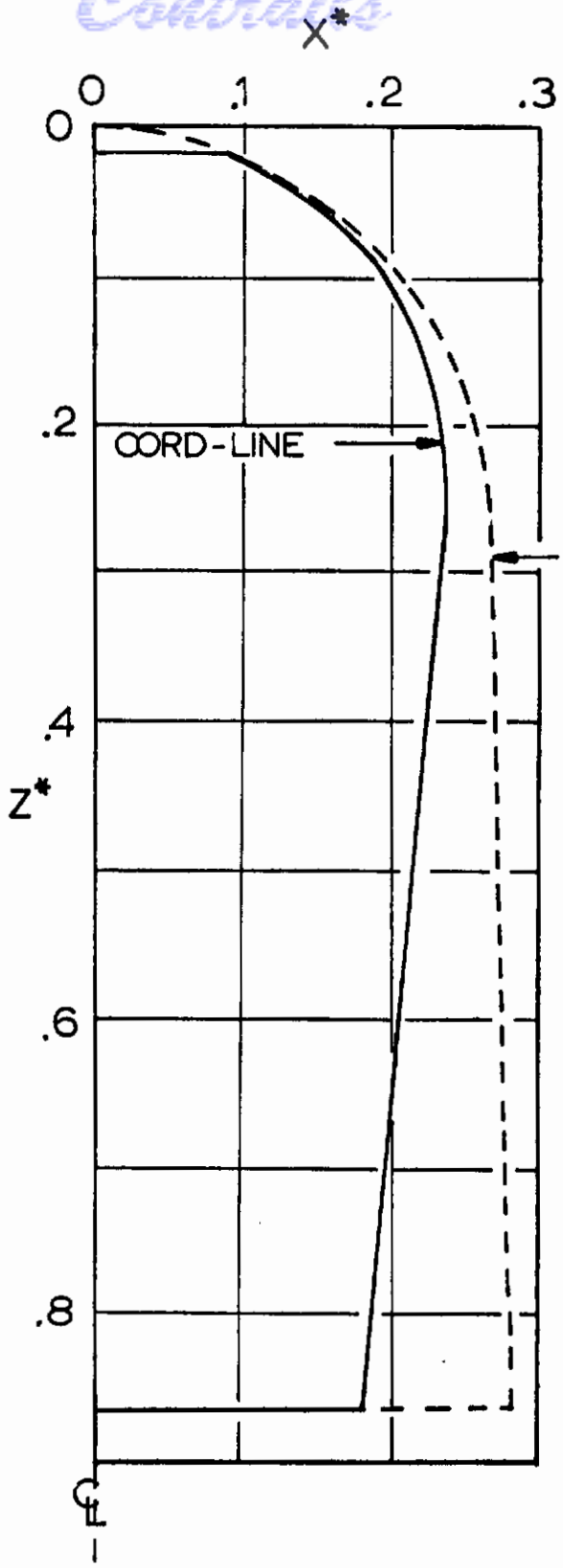

$X^* = \frac{X}{D_o/2}$

$Z^* = \frac{Z}{D_o/2}$

SOLID FLAT CANOPY

$\frac{D_c}{D_o} = 0.239$

$\frac{D_v}{D_o} = 0.10$

N = 28

FIG 9 PROFILE SHAPE OF RIGID MODEL 2

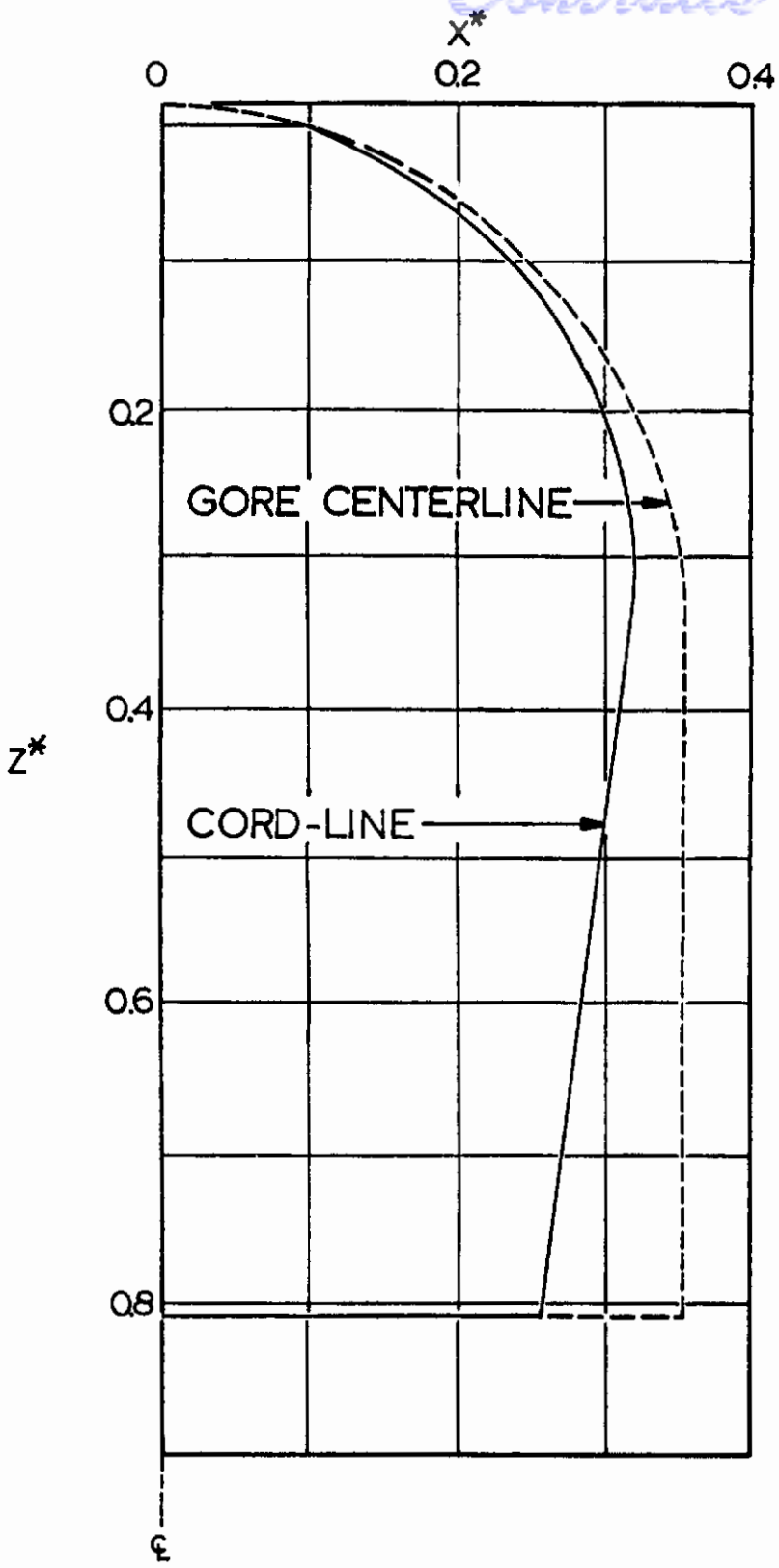

FIG 10 PROFILE SHAPE OF RIGID MODEL 3

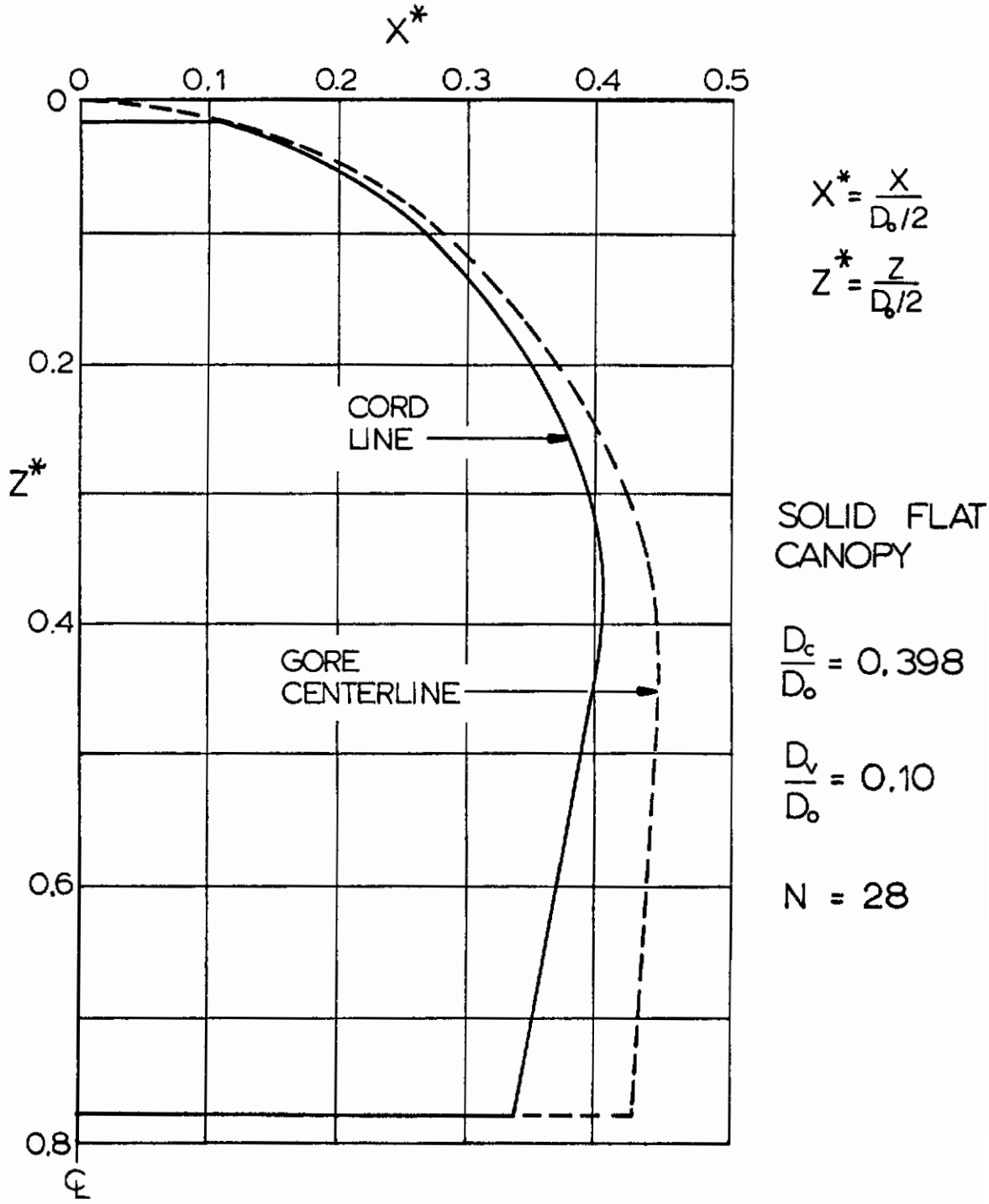

FIG 11. PROFILE SHAPE OF RIGID MODEL 4

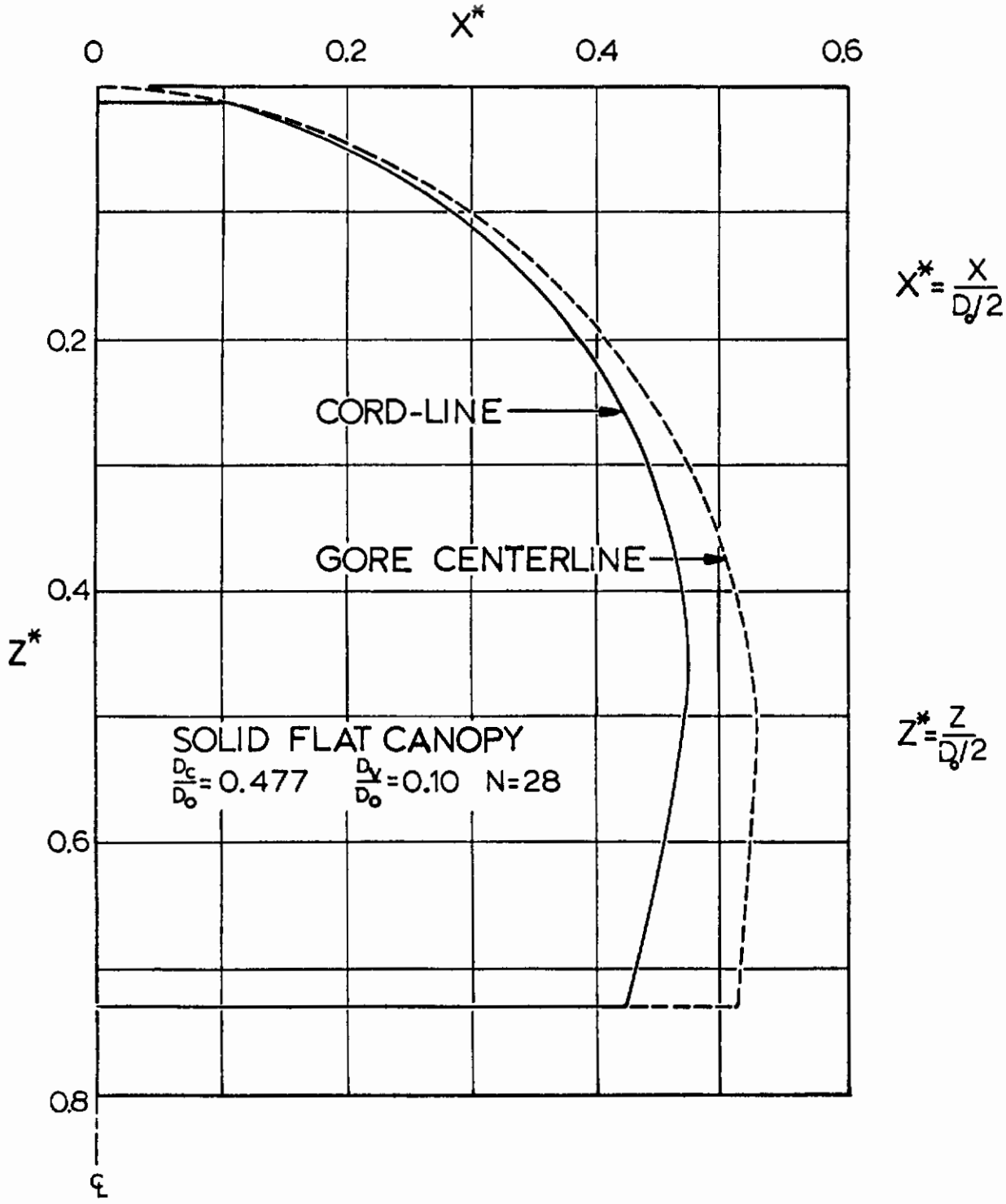

FIG 12 PROFILE SHAPE OF RIGID MODEL 5

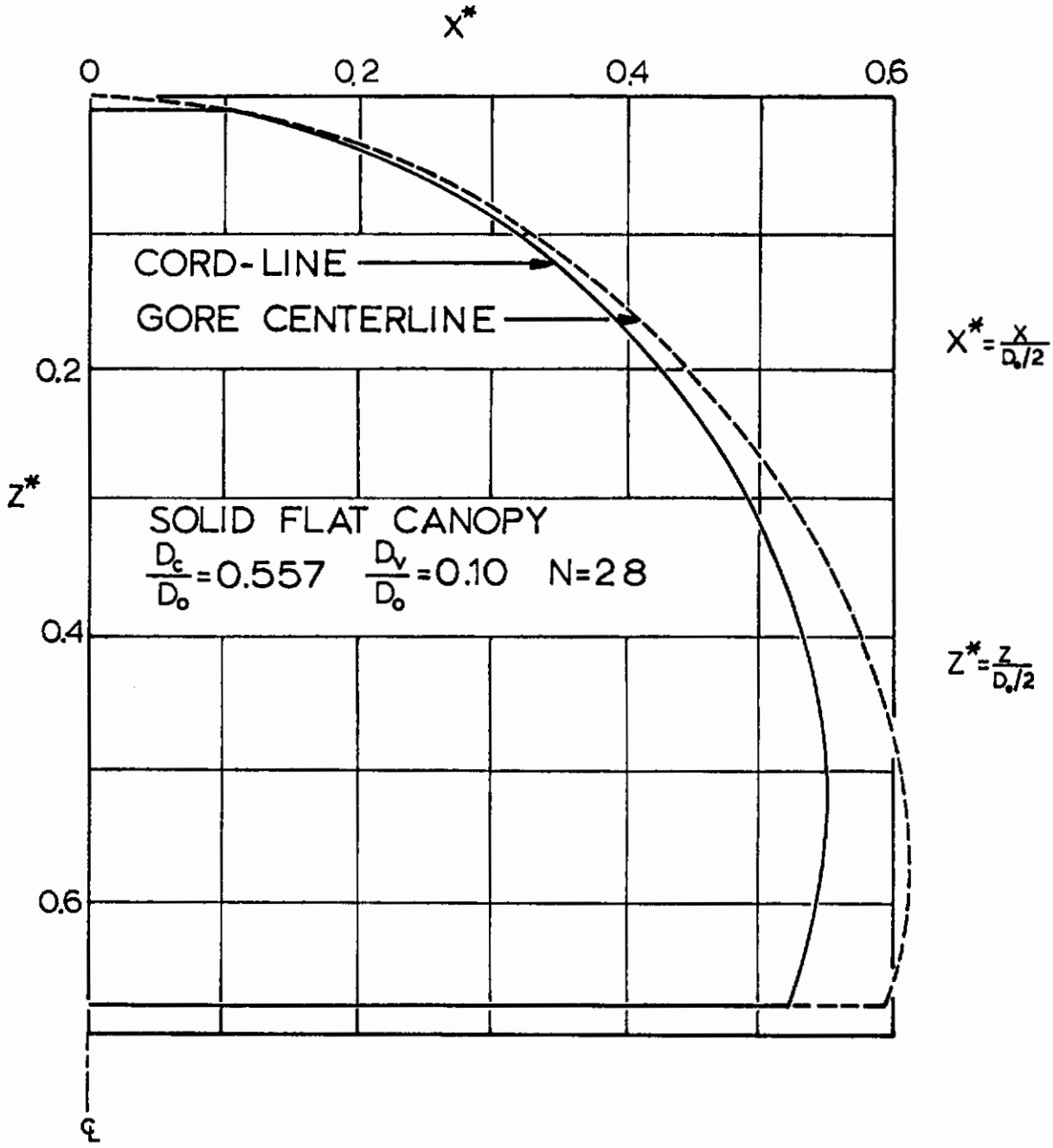

FIG 13 PROFILE SHAPE OF RIGID MODEL 6

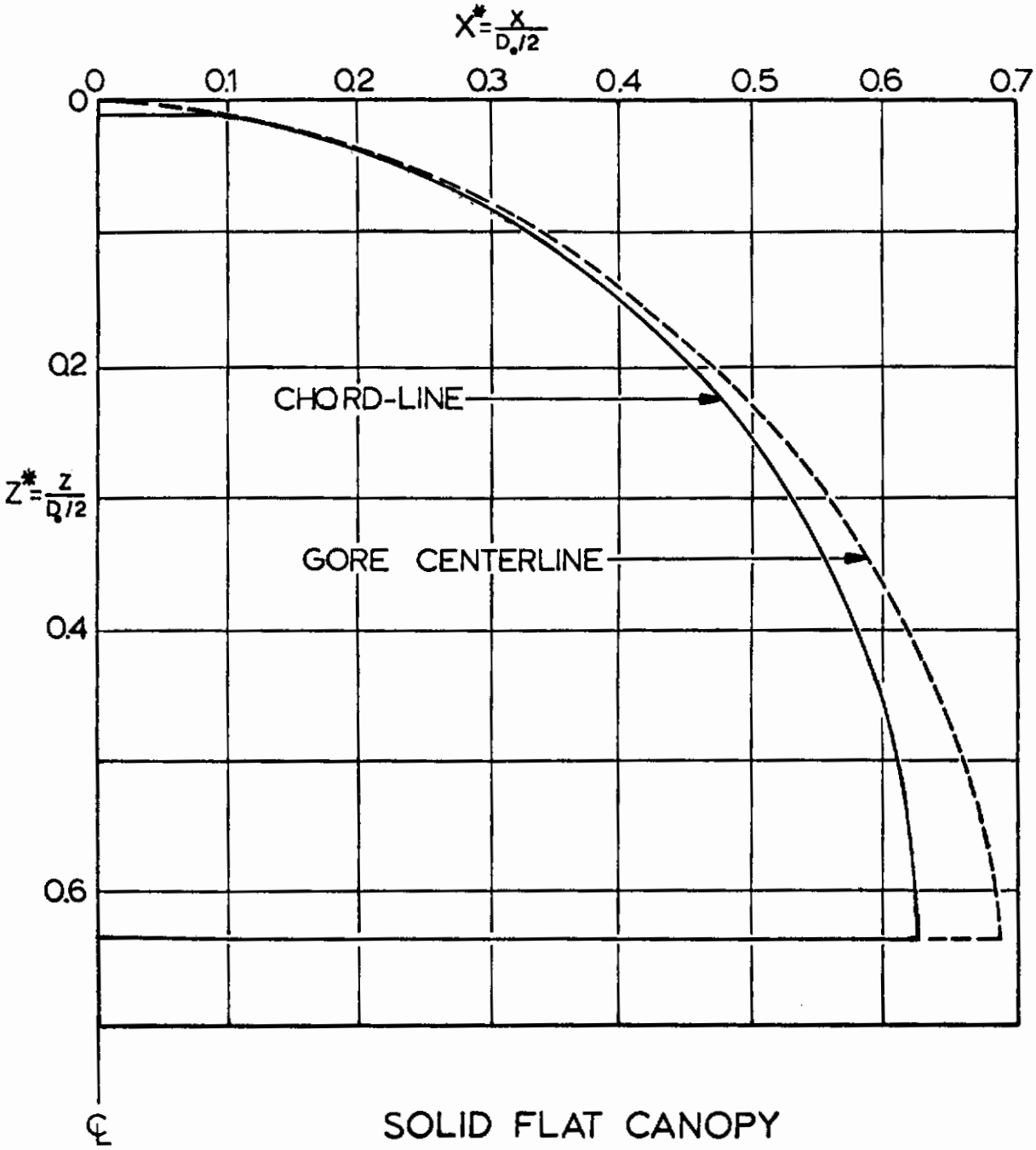

FIG. 14 PROFILE SHAPE OF RIGID MODEL 7

evident that in principle both methods are identical. It is merely a matter of convenience which method one chooses to pursue.

For further convenience in the calculation, the pressure distribution of the various shapes as shown in Ref 10 have been replotted as a function of the length of the cord lines, s_c^*. The results are shown in Fig 15.

The described parachute model was then used to obtain velocity-diameter-time relationships which are necessary to calculate the parameter λ^*. For this purpose the parachute model was suspended in the subsonic wind tunnel of the University of Minnesota and was free to move downstream along a centrally suspended guide wire. The model was connected to a weight of 1.71 lbs which by means of a pulley arrangement was pulled horizontally along a track mounted on top of the wind tunnel. The canopy loading amounted to $W_s/D_o = 0.242$ lb/ft^2. In this experimental setup, the instantaneous values of velocity, size and force were recorded by means of a high speed camera coupled with force sensing elements and a Century oscillograph.

The results of the velocity and the size measurements are shown in Figs 16 and 17 in which the symbols V and D represent, respectively, the instantaneous values of velocity and projected diameter. With this information available one can calculate λ^* from

$$\lambda^* = \tfrac{1}{2}\,\rho V^2 C_p \,\frac{D_o/2}{E}\,\tan\frac{\pi}{N} \quad . \tag{24}$$

This process has been carried through and λ^* is shown as a function of the lengths of the cord line in Fig 18.

The strain, ε, versus the length of the cord line, s_c^*, can be determined as shown in Figs 19 through 25. Under the assumption of perfect elasticity the stress is merely a multiple of the strain and the strain presentations may be taken as characteristic for the stress distribution.

The strain curves can now be evaluated for various purposes. For example, one may want to establish the magnitude and location of the maximum stress during the process of opening. The strain curves also reveal that, particularly in the early stages, the strain or stress is highest in the central portion of the canopy. Further, one

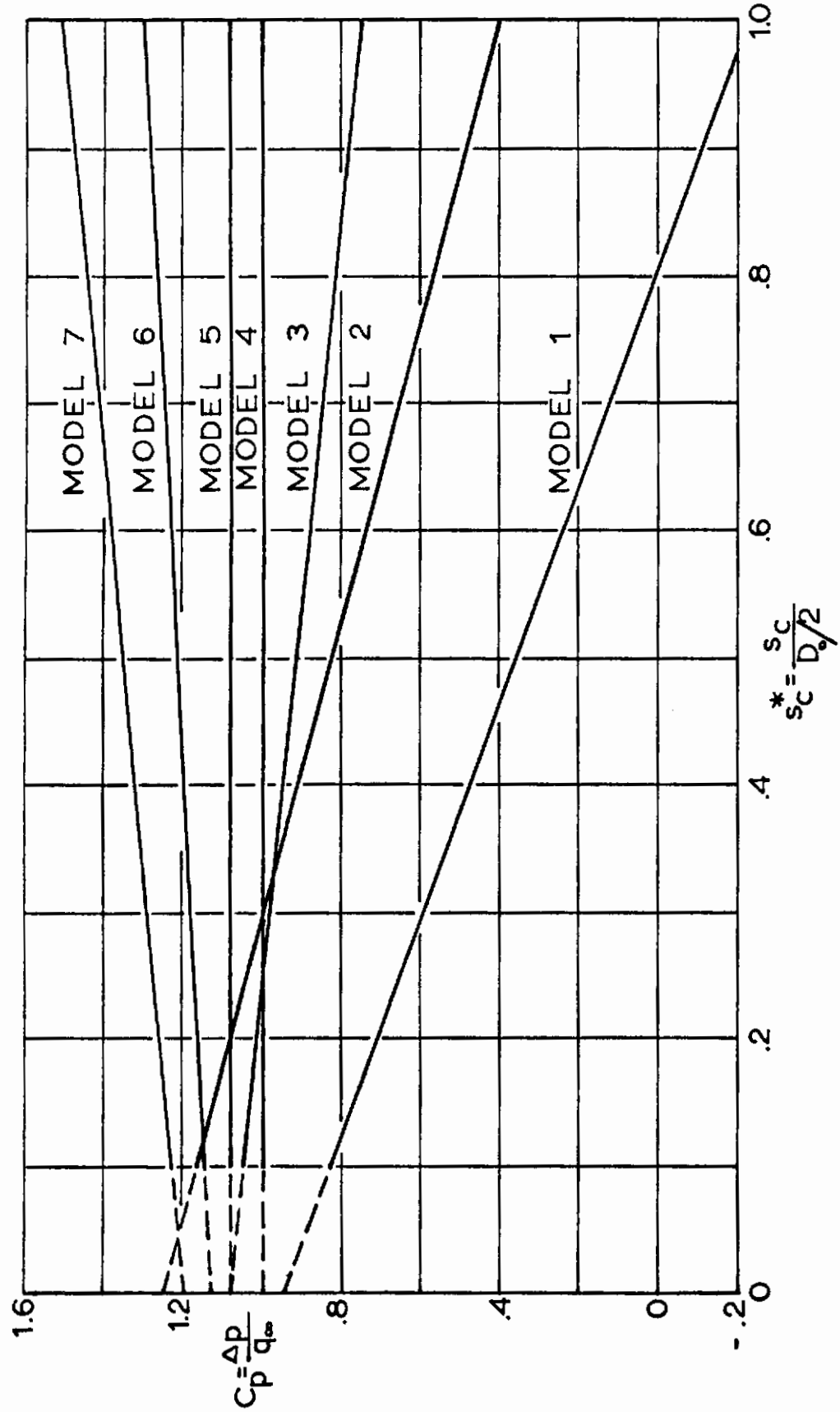

FIG 15 - PRESSURE COEFFICIENT VERSUS LOCATION ON CANOPY FOR RIGID MODELS 1 THROUGH 7.

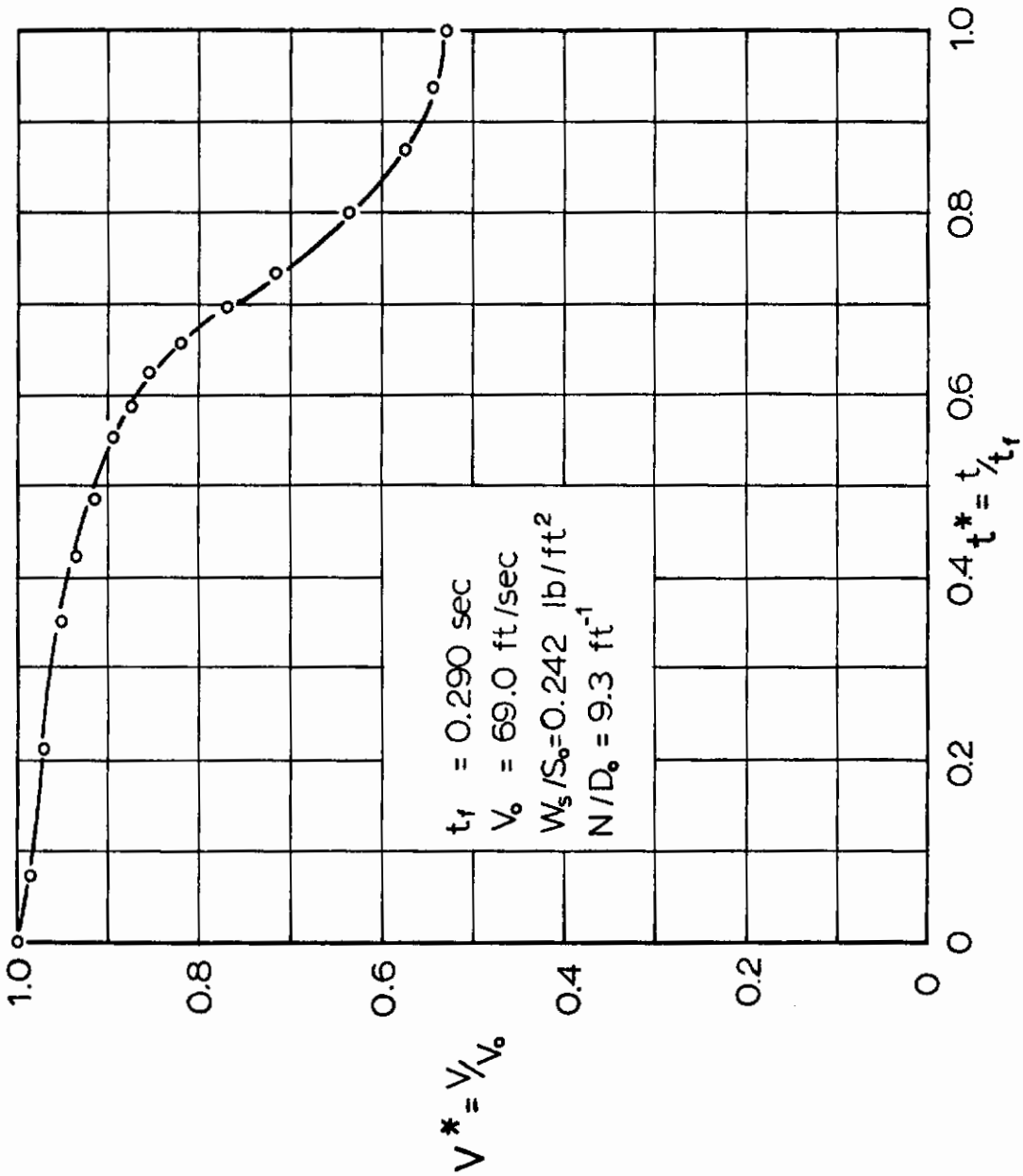

FIG 16 DIMENSIONLESS VELOCITY RATIO - TIME HISTORY FOR AN OPENING SOLID FLAT CANOPY

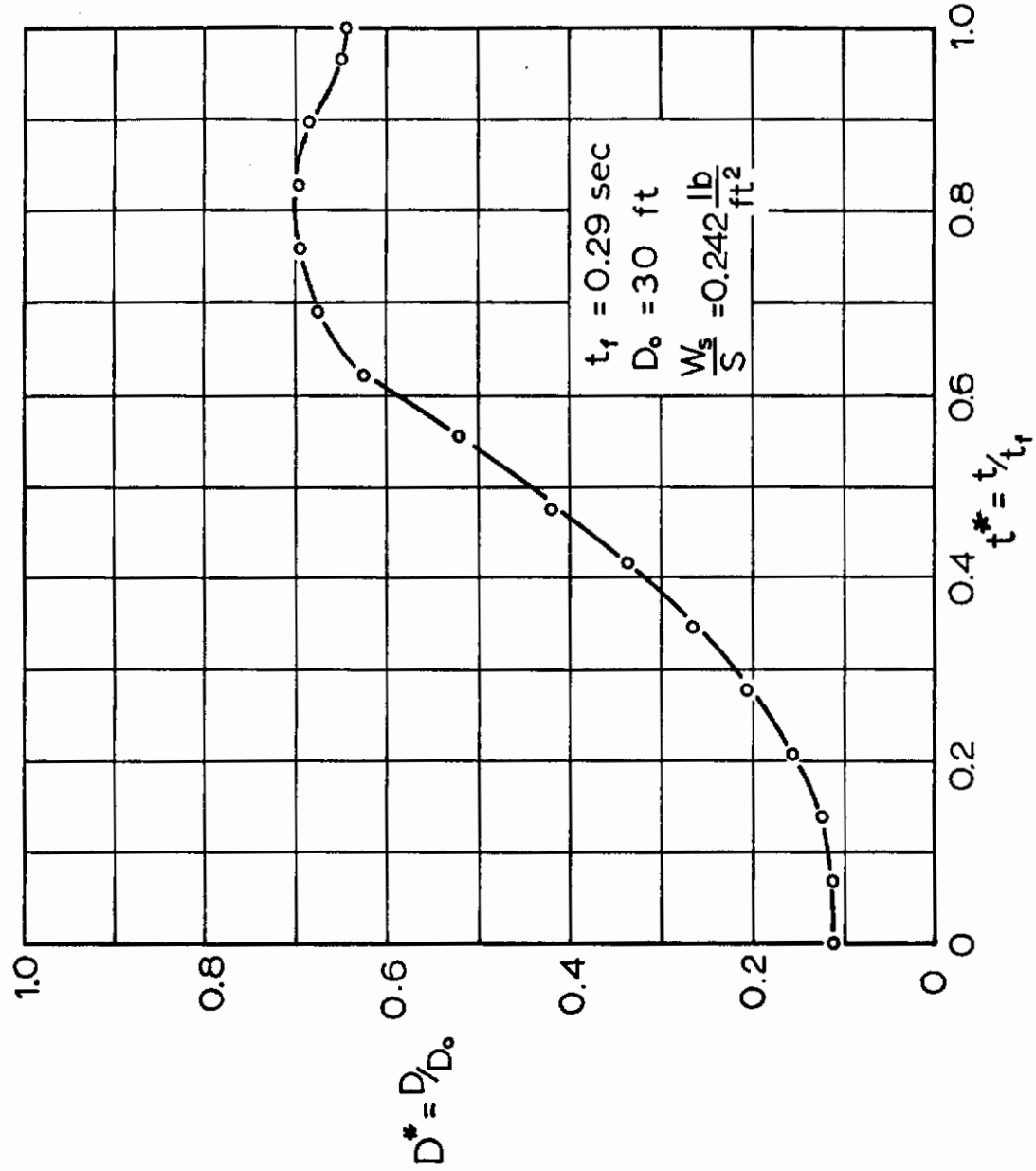

FIG17. DIMENSIONLESS DIAMETER RATIO - TIME HISTORY FOR AN OPENING SOLID FLAT CANOPY

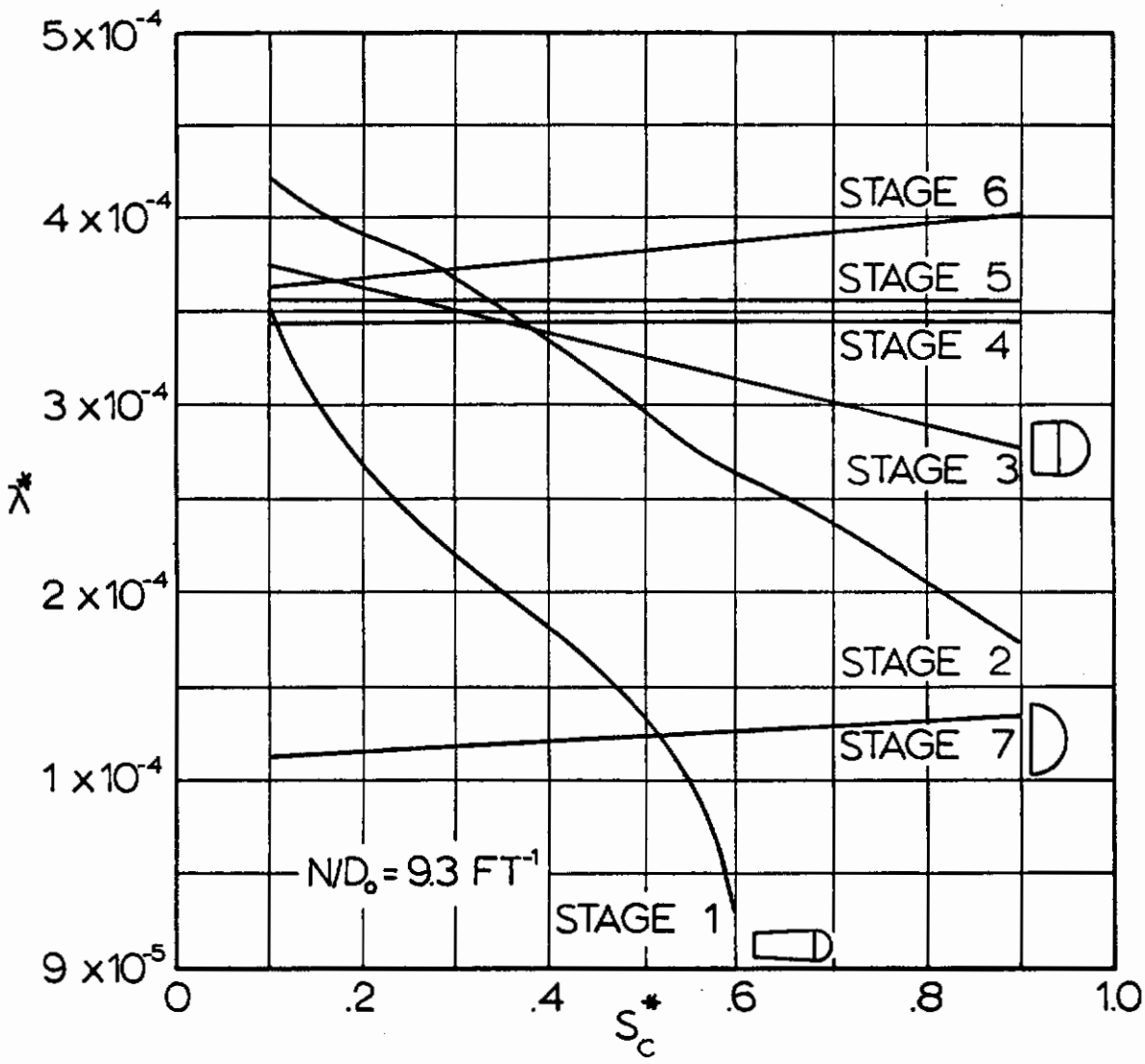

FIG 18. THE DIMENSIONLESS PARAMETER λ^* VERSUS LOCATION ON THE CANOPY FOR SEVEN OPENING STAGES OF THE FLEXIBLE MODEL

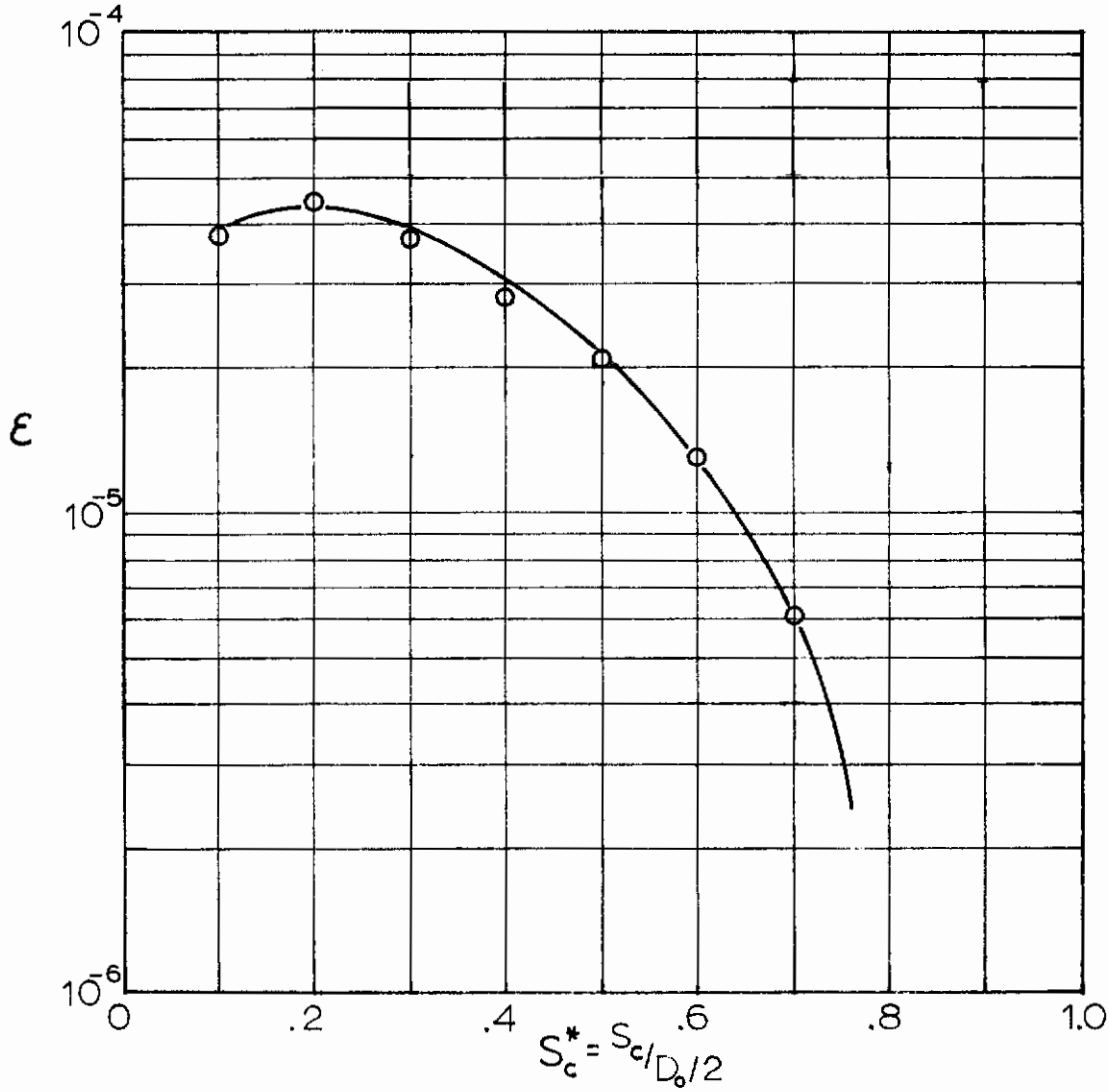

FIG 19 STRAIN vs LOCATION ON CANOPY
(OPENING STAGE 1 , $t^* = 0.215$)

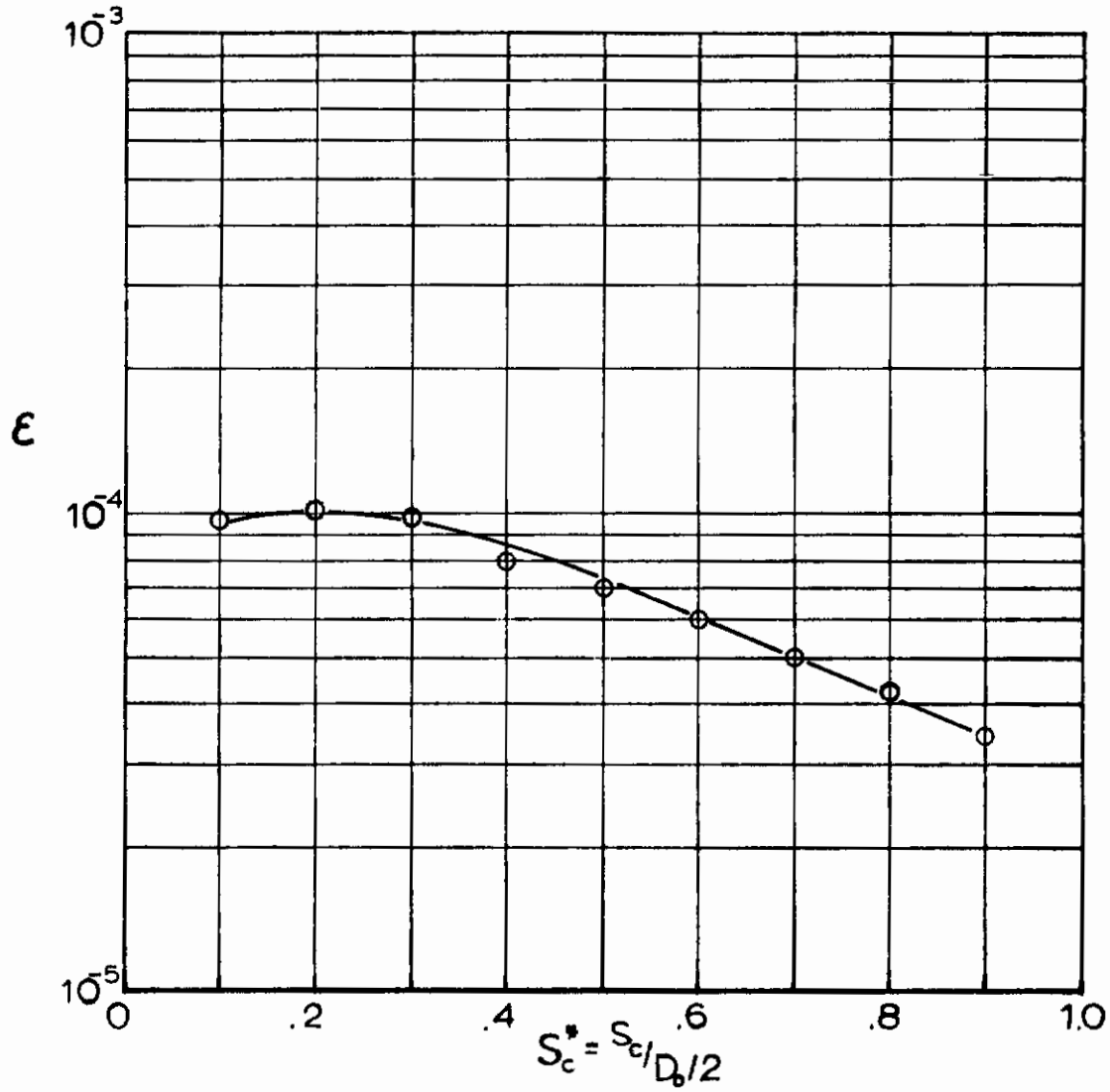

FIG 20. STRAIN vs LOCATION ON CANOPY (OPENING STAGE 2, $t^* = 0.315$)

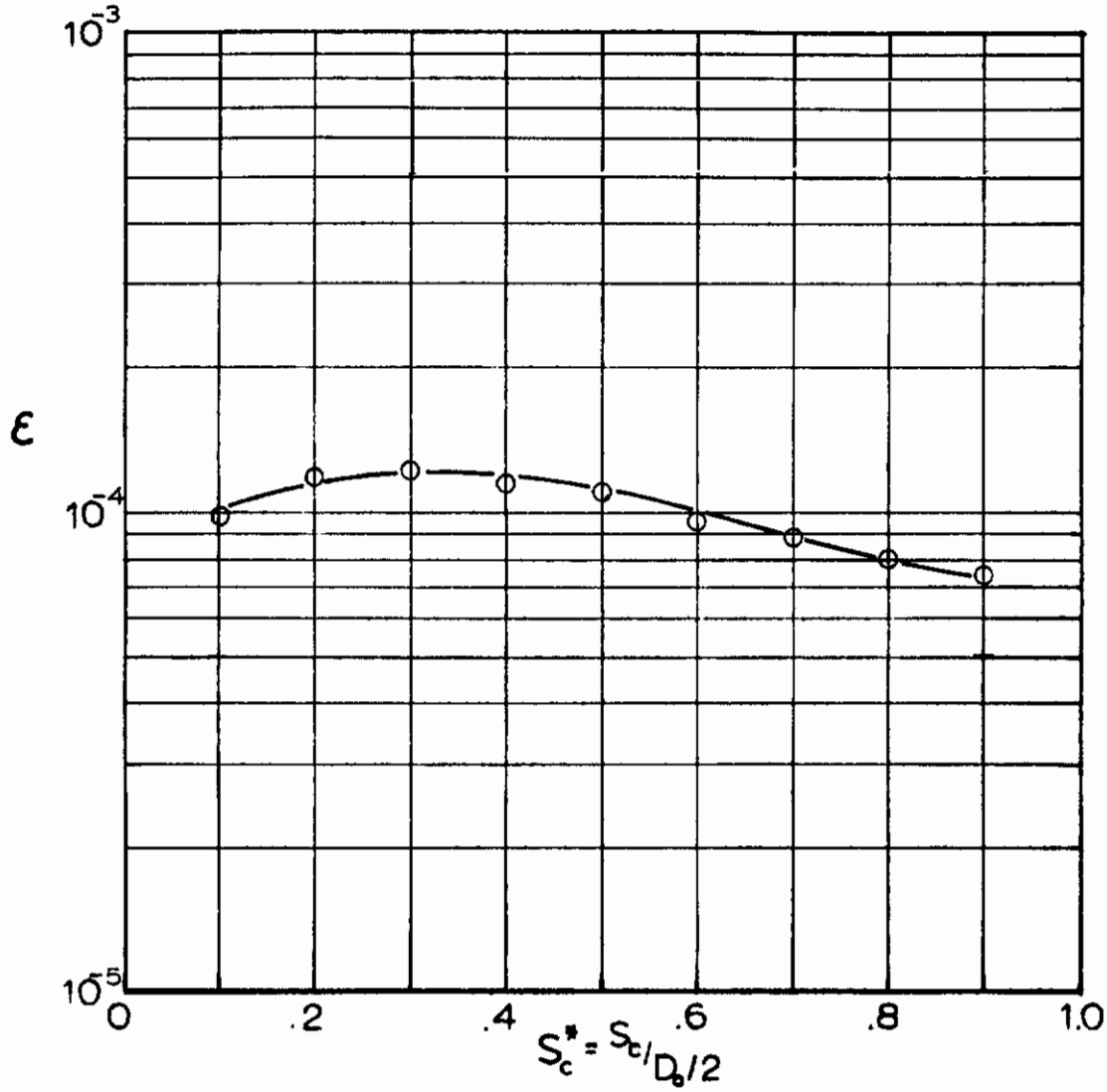

FIG 21. STRAIN vs LOCATION ON CANOPY (OPENING STAGE 3, $t^* = 0.400$)

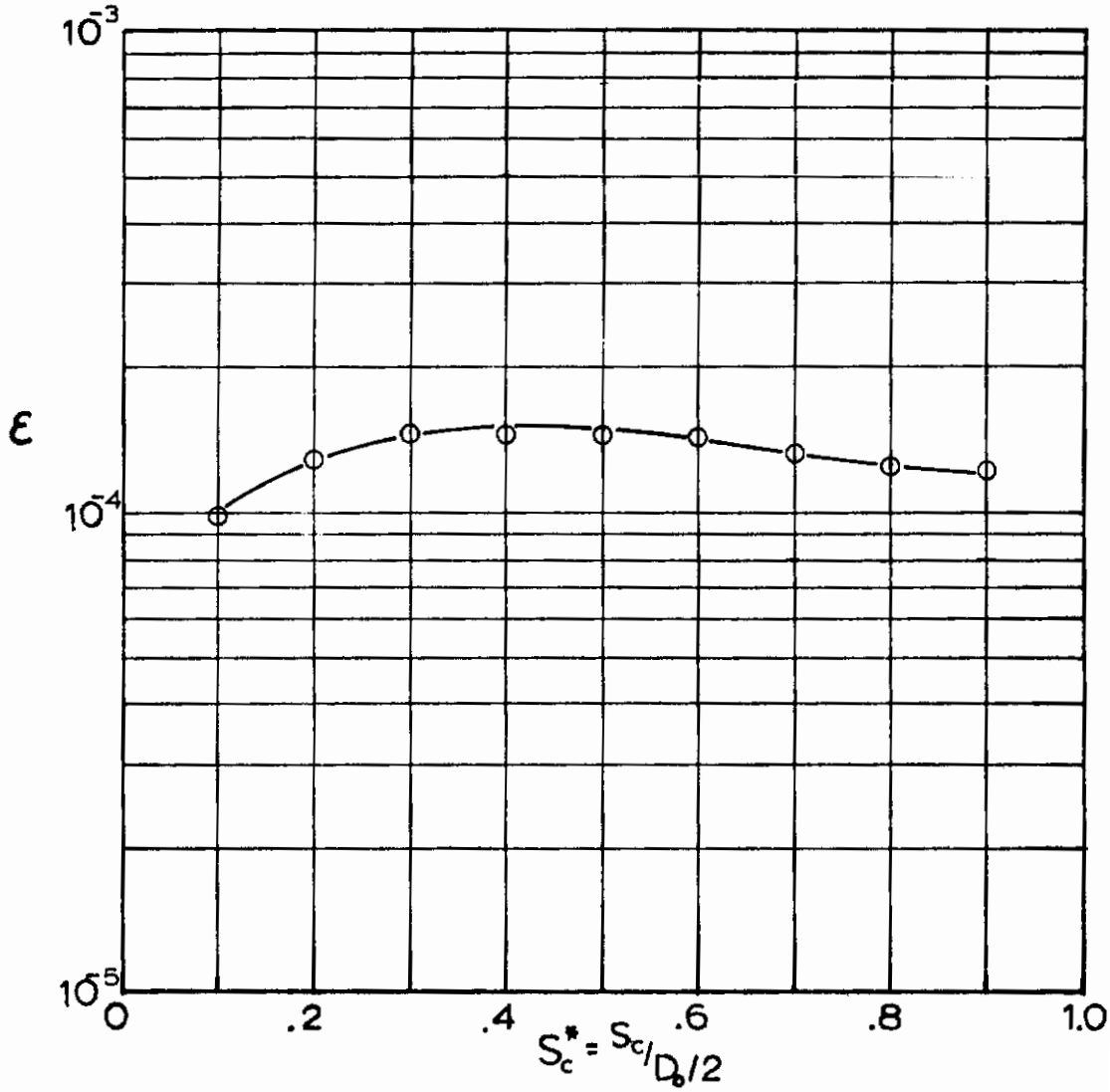

FIG 22. STRAIN vs LOCATION ON CANOPY (OPENING STAGE 4, $t^* = 0.465$)

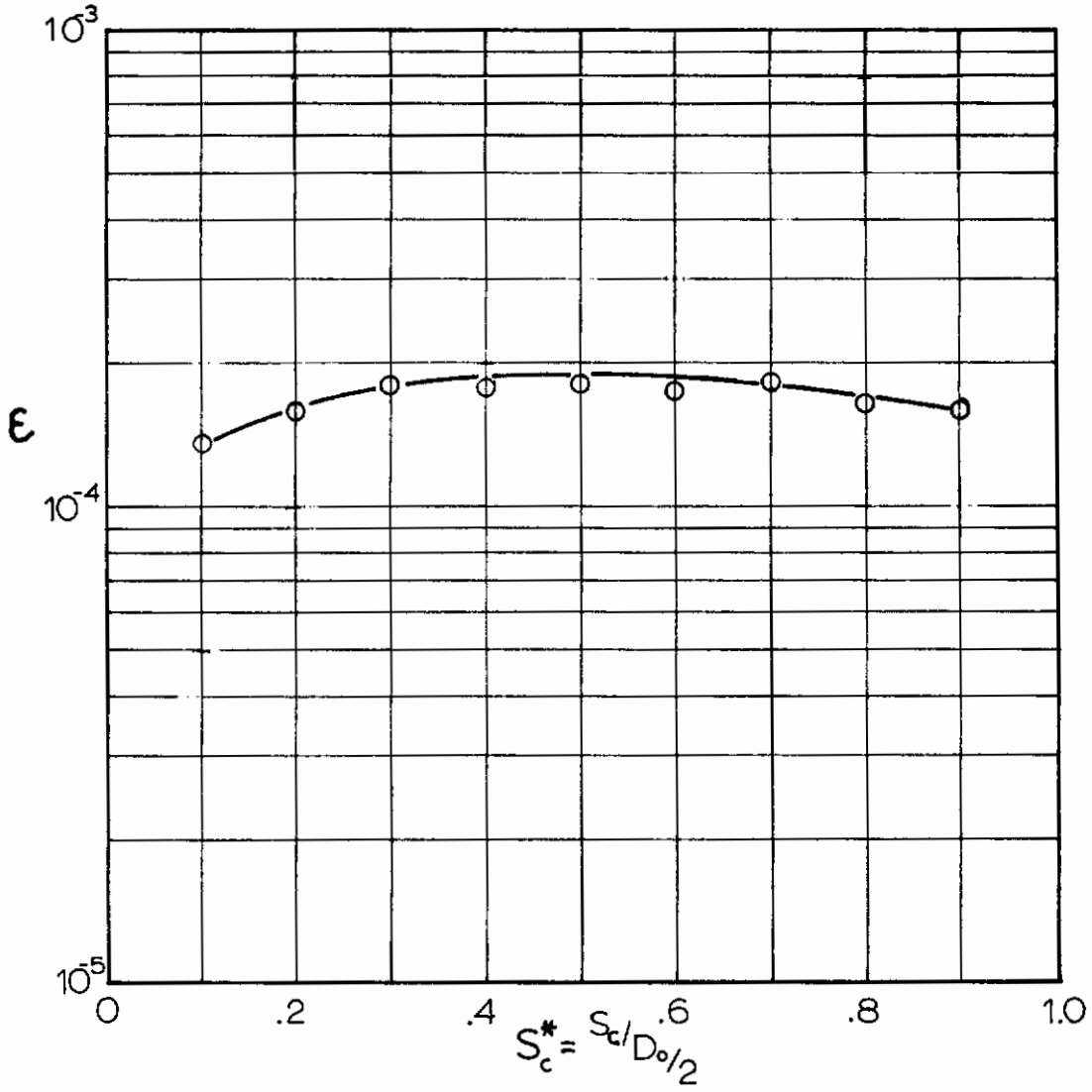

FIG 23. STRAIN vs LOCATION ON CANOPY
(OPENING STAGE 5 $t^* = 0.525$)

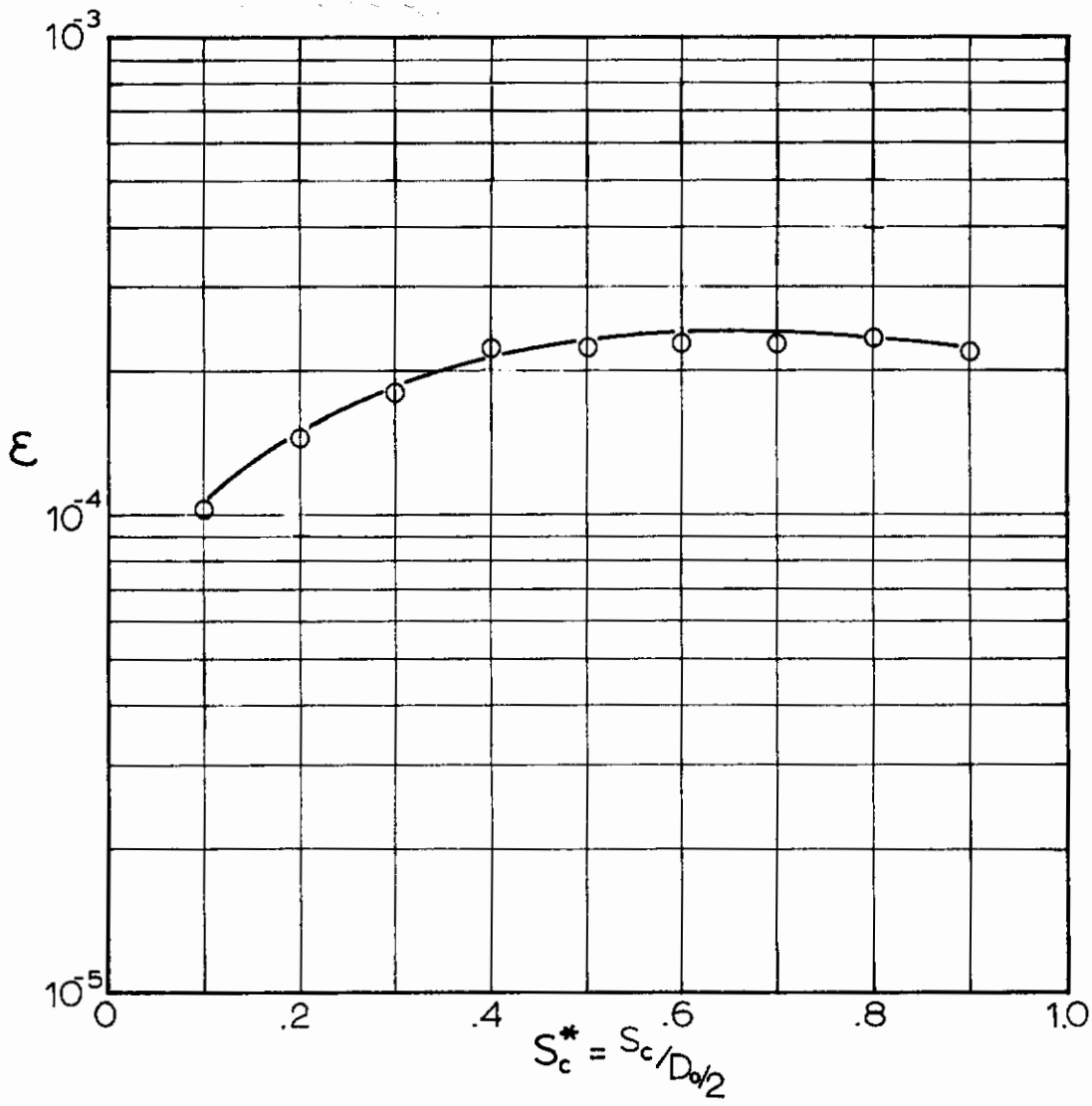

FIG 24. STRAIN vs LOCATION ON CANOPY (OPENING STAGE 6, $t^* = 0.570$)

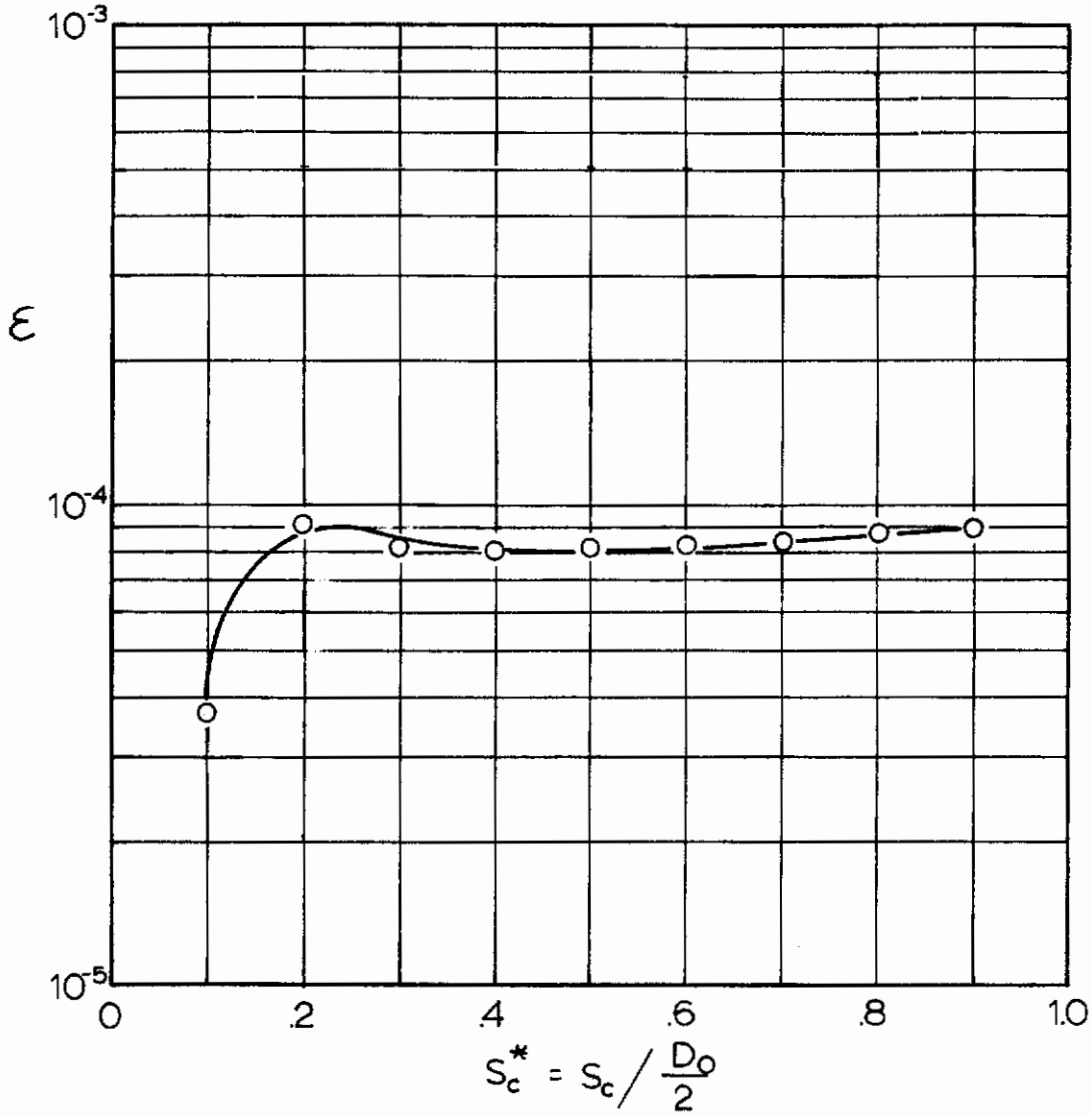

FIG 25 STRAIN vs LOCATION ON CANOPY
(OPENING STAGE 7 $t^* = 1.00$)

will notice that the point of the highest strain moves toward the skirt of the canopy as the inflation process approaches its completion. In the case of opening stage No. 1, the strain even reverses theoretically to negative values which is a consequence of the pressure distribution of this idealized stage showing a resulting pressure from the outer to the inner surface (Ref 10).

In concluding this discussion, one should realize that the presented method assumes that all of the canopy cloth bulges outwardly in between the suspension lines in circular arcs. This is certainly a very questionable assumption, particularly for the skirt region during the early stages of inflation, and one may consider the calculated stresses near the skirt as somewhat unrealistic. However, in the center portions of the canopy where one may assume a regular bulging of cloth, this assumption is quite good and the stress calculation may be considered to be a good approximation. These stresses are also the more important ones since they are higher than the theoretically possible stresses near the skirt.

For the same reason the stress calculation concerning the portions near the skirt become more realistic as the canopy approaches its state of full inflation.

In view of these facts one could limit the presented stress calculations to the more central portions of the canopy, particularly for the early stages of inflation. As the inflation progresses, one should extend the calculation gradually toward the skirt portion of the canopy. This method would be less time consuming than a complete stress analysis and would probably be just as useful.

REFERENCES

1. Jones, R.: On the Aerodynamic Characteristics of Parachutes, R. & M. No. 862, June, 1923.

2. Stevens, G. W. H. and Johns, T. F.: The Theory of Parachutes With Cords Over the Canopy, R. & M. No. 2320, July, 1942.

3. Duncan, W. J., Stevens, G. W. H. and Richards, G. J.: Theory of the Flat Elastic Parachute, R. & M. No. 2118, March, 1942.

4. Beck, E.: The Parachute Considered as a Flexible Shell of Rotation, USAF Translation No. F-TS-3630-Re-BR-281 of German Report, ATI 32297, November, 1942.

5. Reagan, J. F.: A Theoretical Investigation into the Dynamics and Stress Analysis of Parachutes for the Purpose of Determining Design Factors, Daniel Guggenheim Airship Institute Report No. 130, February, 1945.

6. Topping, A. D., Marketos, J. D. and Costakos, N. C.: A Study of Canopy Shapes and Stresses for Parachutes in Steady Descent, WADC TR 55-294, Goodyear Aircraft Corporation, October, 1955.

7. O'Hara, F.: Notes on the Opening Behaviour and the Opening Forces of Parachutes, J. Roy. Aero. Soc. 53 (1949), pp. 1053-1062.

8. Monson, Daryl J.: Stress Analysis of an Opening Parachute Canopy, Master's Thesis submitted to the Graduate School of the University of Minnesota, January, 1963.

9. Heinrich, H. G.: Guide Surface Parachute, ASTIA Document ATI 28935, February 10, 1948.

10. Performance of and Design Criteria for Deployable Aerodynamic Decelerators, ASD-TR-61-579, December, 1963.

APPENDIX I

DERIVATIONS OF EQUATIONS 7 AND 19

1. Derivation of Equation 7 for the Length, b_o

It is given that:

$$y = 2\, r_{b_o} \left(\alpha_o - \frac{\alpha_o^3}{3!} \right) , \tag{1}$$

$$d_o = 2\, r_{b_o}\, \alpha_o , \tag{2}$$

$$b_o = r_{b_o} \left(\frac{\alpha_o^2}{2!} - \frac{\alpha_o^4}{4!} \right) , \tag{3}$$

$$d_o = 2\, s_g \tan \frac{\pi}{N} \tag{4}$$

and

$$y = 2\, x_c \tan \frac{\pi}{N} \tag{5}$$

Introduce Eqns 5 and 2 into Eqn 1 to give:

$$2\, x_c \tan \frac{\pi}{N} = d_o \left(1 - \frac{\alpha_o^2}{6} \right) . \tag{1-A}$$

Into this, introduce Eqn 4 to give:

$$x_c = s_g \left(1 - \frac{\alpha_o^2}{6} \right) ,$$

or,

$$\alpha_o = \sqrt{6} \left(1 - \frac{x_c}{s_g} \right)^{\frac{1}{2}} . \tag{2-A}$$

Combining Eqn 2 with Eqn 3 provides:

$$b_o = \frac{d_o}{2} \left(\frac{\alpha_o}{2} - \frac{\alpha_o^3}{24} \right) . \tag{3-A}$$

Equation 4 makes this

$$b_o = s_g \tan \frac{\pi}{N} \left(\frac{\alpha_o}{2} - \frac{\alpha_o^3}{24} \right) . \qquad (4\text{-A})$$

Substitute Eqn 2-A into Eqn 4-A to eliminate α_o. There results:

$$b_o = \left(\frac{s_g \tan \frac{\pi}{N}}{2}\right) \sqrt{6} \left(1 - \frac{x_c}{s_g}\right)^{\frac{1}{2}} \left[1 - \tfrac{1}{2} \left(1 - \frac{x_c}{s_g}\right)\right]$$

or

$$b_o = \frac{\sqrt{6}\, s_g \tan \frac{\pi}{N}}{4} \left(1 - \frac{x_c}{s_g}\right)^{\frac{1}{2}} \left[\frac{x_c}{s_g} + 1\right]$$

or

$$b_o = \frac{\sqrt{6} \tan \frac{\pi}{N}}{4 \sqrt{s_g}} \left(s_g - x_c\right)^{\frac{1}{2}} \left(s_g + x_c\right). \qquad (7)$$

2. Derivation of Equation 19 for the Stress, f
It is given that:

$$y = 2 r_b \left(\alpha - \frac{\alpha^3}{6} \right) , \qquad (1)$$

$$d = 2 r_b \alpha , \qquad (2)$$

$$f_1 = \Delta p \, r_b , \qquad (16)$$

$$d_o = 2 s_g \tan \frac{\pi}{N} , \qquad (4)$$

$$y = 2 x_c \tan \frac{\pi}{N} , \qquad (5)$$

$$f_1 = E \varepsilon , \qquad (17)$$

$$d = (1 + \varepsilon) d_o . \qquad (18)$$

Introduce Eqns 2 and 5 into Eqn 1 to give

$$x_c \tan \frac{\pi}{N} = \frac{d}{2} - \frac{d^3}{48 r_b^2} \quad . \tag{5-A}$$

From Eqns 4, 17 and 18 it is seen that

$$d = 2 s_g \tan \frac{\pi}{N} \left(1 + \frac{f_1}{E}\right) . \tag{6-A}$$

Introducing Eqns 16 and 6-A into Eqn 5-A to eliminate r_b and d, respectively, provides:

$$x_c = s_g \left(1 + \frac{f_1}{E}\right) - \frac{1}{6} \tan^2 \frac{\pi}{N} (\Delta p)^2 \frac{s_g^3}{f_1^2} \left(1 + \frac{f_1}{E}\right)^3 \tag{7-A}$$

Expanding the terms makes this

$$x_c f_1^2 = s_g f_1^2 + \frac{s_g}{E} f_1^3 - \frac{1}{6} \tan^2 \frac{\pi}{N} (\Delta p)^2 s_g^3 \left[1 + \right.$$

$$\left. + \frac{3}{E} f_1 + \frac{3}{E^2} f_1^2 + \frac{1}{E^3} f_1^3 \right] . \tag{8-A}$$

Combining common terms provides:

$$\left[\frac{s_g}{E} - \frac{1}{6} \tan^2 \frac{\pi}{N} (\Delta p)^2 \frac{s_g^3}{E^3}\right] f_1^3 + \left[s_g - x_c - \tfrac{1}{2} \tan^2 \frac{\pi}{N} (\Delta p)^2 \frac{s_g^3}{E^2}\right] f_1^2 -$$

$$- \left[\tfrac{1}{2} \tan^2 \frac{\pi}{N} (\Delta p)^2 \frac{s_g^3}{E}\right] f_1 - \left[\frac{1}{6} \tan^2 \frac{\pi}{N} (\Delta p)^2 s_g^3\right] = 0,$$

or

$$f_1^3 + \left[\frac{6\,E^2\,(1 - \frac{x_c}{s_g}) - 3E\,(\tan \frac{\pi}{N}\,\Delta p\, s_g)^2}{6\,E^2 - (\tan \frac{\pi}{N}\,\Delta p\, s_g)^2} \right] f_1^2$$

$$- \left[\frac{3E^2\,(\tan \frac{\pi}{N}\,\Delta p\, s_g)^2}{6E^2 - (\tan \frac{\pi}{N}\Delta p\, s_g)^2} \right] f_1 - \left[\frac{E^3\,(\tan \frac{\pi}{N}\,\Delta p\, s_g)^2}{6E^2 - (\tan \frac{\pi}{N}\,\Delta\, p\, s_g)^2} \right] = 0. \qquad (19)$$

Unclassified

Security Classification

DOCUMENT CONTROL DATA - R&D

(Security classification of title, body of abstract and indexing annotation must be entered when the overall report is classified)

1. ORIGINATING ACTIVITY *(Corporate author)* RTD WPAFB, Ohio	2a. REPORT SECURITY CLASSIFICATION Unclassified 2b. GROUP n/a

3. REPORT TITLE

Stress Analysis of a Parachute During Inflation and at Steady State

4. DESCRIPTIVE NOTES *(Type of report and inclusive dates)*

Final Report 15 April 1963 - 1 August 1964

5. AUTHOR(S) *(Last name, first name, initial)*

Jamison, Lelan R., Jr.
Heinrich, Helmut G.

6. REPORT DATE February 1965	7a. TOTAL NO. OF PAGES 46	7b. NO. OF REFS 10
8a. CONTRACT OR GRANT NO. AF33(657)-11184 b. PROJECT NO. 6065 c. 606503 d.	9a. ORIGINATOR'S REPORT NUMBER(S) FDL-TDR-64-125 9b. OTHER REPORT NO(S) *(Any other numbers that may be assigned this report)* none	

10. AVAILABILITY/LIMITATION NOTICES

Qualified requesters may obtain copies of this report from DDC.
DDC release to CFSTI is not authorized.

11. SUPPLEMENTARY NOTES n/a	12. SPONSORING MILITARY ACTIVITY AFFDL (FDFR) WPAFB, Ohio

13. ABSTRACT

The stresses occurring in the cloth of an opening parachute and at steady state are calculated. The method is based on assumed instantaneous and steady state shapes and related pressure distributions. It is general and may be applied to any type and size of canopy built out of solid cloth. The presented analysis is limited to canopies constructed of triangular gores, but can be extended to other gore patterns. A numerical calculation is made for the Solid Flat, Circular Parachute during the opening and at steady state.

DD FORM 1 JAN 64 1473

Unclassified

Security Classification

14. KEY WORDS	LINK A		LINK B		LINK C	
	ROLE	WT	ROLE	WT	ROLE	WT
Numerical Calculation Solid Cloth Parachute Stress Distribution over Surface Triangular Gore Pattern Pressure Distribution						

INSTRUCTIONS

1. ORIGINATING ACTIVITY: Enter the name and address of the contractor, subcontractor, grantee, Department of Defense activity or other organization *(corporate author)* issuing the report.

2a. REPORT SECURITY CLASSIFICATION: Enter the overall security classification of the report. Indicate whether "Restricted Data" is included. Marking is to be in accordance with appropriate security regulations.

2b. GROUP: Automatic downgrading is specified in DoD Directive 5200.10 and Armed Forces Industrial Manual. Enter the group number. Also, when applicable, show that optional markings have been used for Group 3 and Group 4 as authorized.

3. REPORT TITLE: Enter the complete report title in all capital letters. Titles in all cases should be unclassified. If a meaningful title cannot be selected without classification, show title classification in all capitals in parenthesis immediately following the title.

4. DESCRIPTIVE NOTES: If appropriate, enter the type of report, e.g., interim, progress, summary, annual, or final. Give the inclusive dates when a specific reporting period is covered.

5. AUTHOR(S): Enter the name(s) of author(s) as shown on or in the report. Enter last name, first name, middle initial. If military, show rank and branch of service. The name of the principal author is an absolute minimum requirement.

6. REPORT DATE: Enter the date of the report as day, month, year; or month, year. If more than one date appears on the report, use date of publication.

7a. TOTAL NUMBER OF PAGES: The total page count should follow normal pagination procedures, i.e., enter the number of pages containing information.

7b. NUMBER OF REFERENCES: Enter the total number of references cited in the report.

8a. CONTRACT OR GRANT NUMBER: If appropriate, enter the applicable number of the contract or grant under which the report was written.

8b, 8c, & 8d. PROJECT NUMBER: Enter the appropriate military department identification, such as project number, subproject number, system numbers, task number, etc.

9a. ORIGINATOR'S REPORT NUMBER(S): Enter the official report number by which the document will be identified and controlled by the originating activity. This number must be unique to this report.

9b. OTHER REPORT NUMBER(S): If the report has been assigned any other report numbers *(either by the originator or by the sponsor)*, also enter this number(s).

10. AVAILABILITY/LIMITATION NOTICES: Enter any limitations on further dissemination of the report, other than those imposed by security classification, using standard statements such as:

(1) "Qualified requesters may obtain copies of this report from DDC."

(2) "Foreign announcement and dissemination of this report by DDC is not authorized."

(3) "U. S. Government agencies may obtain copies of this report directly from DDC. Other qualified DDC users shall request through _____."

(4) "U. S. military agencies may obtain copies of this report directly from DDC. Other qualified users shall request through _____."

(5) "All distribution of this report is controlled. Qualified DDC users shall request through _____."

If the report has been furnished to the Office of Technical Services, Department of Commerce, for sale to the public, indicate this fact and enter the price, if known.

11. SUPPLEMENTARY NOTES: Use for additional explanatory notes.

12. SPONSORING MILITARY ACTIVITY: Enter the name of the departmental project office or laboratory sponsoring *(paying for)* the research and development. Include address.

13. ABSTRACT: Enter an abstract giving a brief and factual summary of the document indicative of the report, even though it may also appear elsewhere in the body of the technical report. If additional space is required, a continuation sheet shall be attached.

It is highly desirable that the abstract of classified reports be unclassified. Each paragraph of the abstract shall end with an indication of the military security classification of the information in the paragraph, represented as *(TS), (S), (C), or (U)*.

There is no limitation on the length of the abstract. However, the suggested length is from 150 to 225 words.

14. KEY WORDS: Key words are technically meaningful terms or short phrases that characterize a report and may be used as index entries for cataloging the report. Key words must be selected so that no security classification is required. Identifiers, such as equipment model designation, trade name, military project code name, geographic location, may be used as key words but will be followed by an indication of technical context. The assignment of links, rules, and weights is optional.